Petroleum Research 8 (2023) 386–403

Contents lists available at ScienceDirect

Petroleum Research

journal homepage: http://www.keaipublishing.com/en/journals/petroleum-research/

Impact of microfacies and diagenesis on the reservoir quality of Upper Devonian carbonates in Southeast Tatarstan, Volga-Ural Basin, Russia

Ibrahem Yousef*, V.P. Morozov, A.N. Kolchugin, A. Leontev

Kazan Federal University, Institute of Geology and Petroleum Technologies, 420008, Russia

ARTICLE INFO

Article history:
Received 6 June 2022
Received in revised form
28 October 2022
Accepted 30 October 2022
Available online 3 November 2022

Keywords:
Microfacies
Diagenesis
Reservoir quality
Upper Devonian
Dankovo-Lebedyansky
Tatarstan
Volga-Ural Basin

ABSTRACT

The results of integrated sedimentology, petrography, and petrophysical study of the Upper Devonian (Middle Famennian) Dankovo-Lebedyansky carbonates from Southeast Tatarstan of the Volga-Ural Basin revealed a variety of microfacies and diagenetic events that impacted the reservoir quality. Although our earlier study documented microfacies analysis and depositional environments, none of the studies focused on diagenesis, microfacies interaction, and their controls on the studied sediment's reservoir quality. Based on petrographic and microfacies analyses, the seven identified microfacies types are peloidal grainstone MF 1, cemented bioclastic peloidal grainstone MF 2, echinoderm-concentrated packstone MF 3, algae packstone MF 4, bioclastic wackestone MF 5, whole-fossil wackestone MF 6, and dolomite MF 7. For the investigated sediments, a gently deepening carbonate ramp depositional model with an inner, middle, and outer ramp setting is proposed. The observed diagenetic events in this study include micritization, calcite cementation (six cement types), dolomitization (six dolomite types), dissolution (fabric and non-fabric-selective dissolution), compaction, and microfracturing. The identified microfacies were classified into three distinct classes based on their petrophysical characteristics. MF 1 and MF 7 are microfacies types with the best reservoir quality. MF 3 and MF 4 are microfacies types of moderate reservoir quality. MF 2, MF 5, and MF 6 are microfacies types with poor or non-reservoir quality. Calcite cementation, micritization, and compaction are the primary diagenetic modifications responsible for porosity reduction. Moldic pores created by dissolution are a significant porosity-improving process. Porosity is locally enhanced by stylolite and microfractures. Dolomitization improved reservoir quality by creating intercrystalline and vuggy porosity. Understanding the impact of microfacies and diagenesis on reservoir quality is crucial for understanding reservoir properties in nearby fields with similar settings.

1. Introduction

The Volga-Ural Basin, or petroleum province (Fig. 1A and B), is one of Russia's major hydrocarbon basins, occupying the eastern part of the East European Platform (Liang et al., 2020; Ibrahem et al., 2022a, b). According to the United States Geological Survey (USGS) (Klett et al., 2018). The Domanik-type formations of the Volga-Ural petroleum province that stratigraphically belong to the Middle Frasnian of the Upper Devonian to the Lower Carboniferous have an estimated mean undiscovered, technically recoverable continuous resources of 2.8 billion barrels of oil and 34 trillion cubic feet of gas. Carbonate rocks, which account for about 70% of the Volga-Ural Basin reservoirs, are significant target facies for oil and gas exploration, production, and development in the basin fields (Morozov et al., 2021; Korshunov and Boguslavskiy, 2022).

The reservoir petrophysical characteristics of carbonate rocks are reported to be controlled by a combination of depositional processes and diagenetic modifications. The depositional processes control the initial pore size distribution and geometry of each depositional facies, whereas the diagenetic processes modify the pore size distribution and control the depositional facies' productivity (Ehrenberg and Nadeau, 2005; Ahr, 2008; Burchette, 2012; Worden et al., 2018; Ahmad et al., 2021).

Evaluations of the relationships between lithofacies, diagenetic modifications, and reservoir quality are highly significant subjects and challenging fields in petroleum geosciences that have long

* Corresponding author.
E-mail address: ibrahem.youseef@mail.ru (I. Yousef).

https://doi.org/10.1016/j.ptlrs.2022.10.006

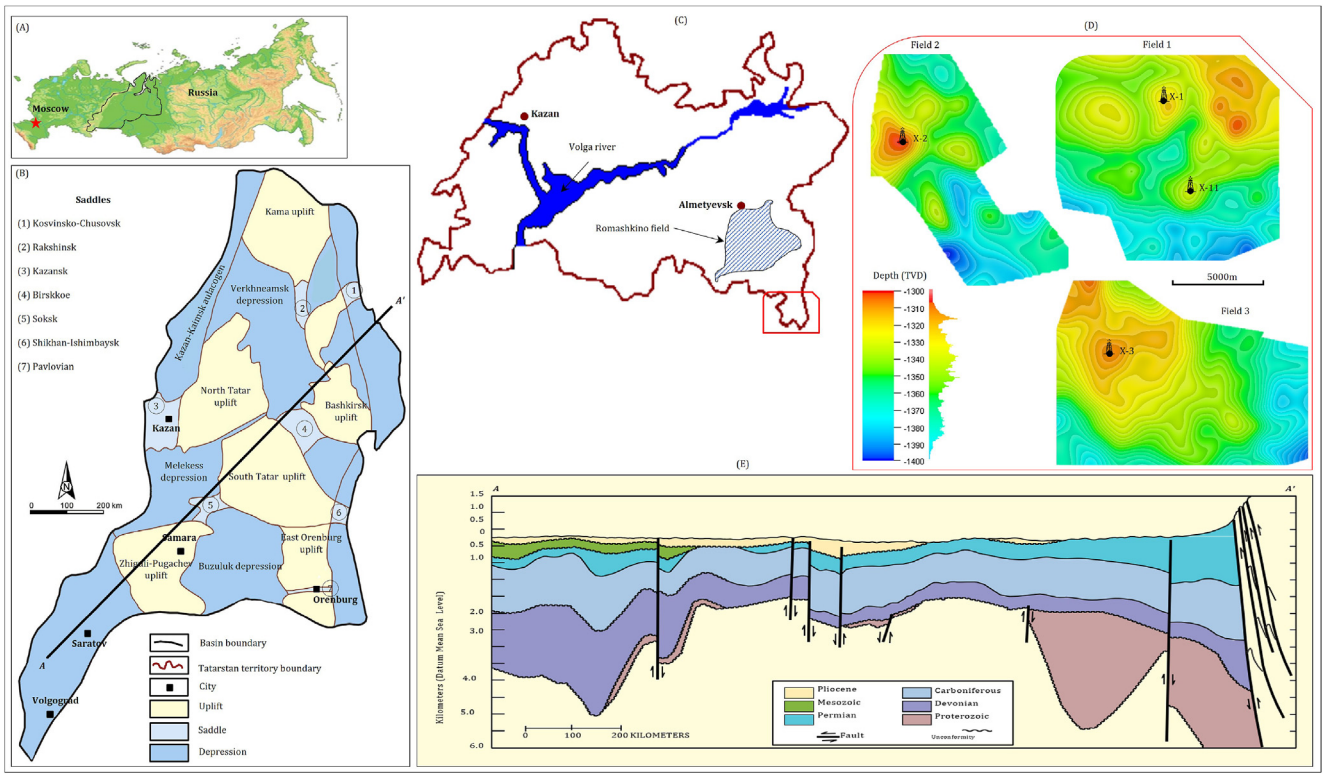

Fig. 1. (A) Map of the Russian territory, showing the boundaries of the Volga-Ural petroleum province. (B) Volga-Ural Basin tectonic units are labeled 1–7 for uplifts, depressions, and saddles (Liang et al., 2020). (C) The study area's location within Tatarstan's territorial boundaries (Ibrahem et al., 2022a). (D) Dankovo-Lebedyansky sediment structural maps in the studied fields, as well as the locations of the studied wells (referred to as X-1, X-2, X-3, and X-4). (E) Cross section A-A' across the of the Volga-Ural Basin (Klett et al., 2018).

been a focus for many academics and petroleum companies. These evaluations are typically more important in carbonate rocks since they are more complicated than clastic reservoirs due to their wide variety of characteristics and are particularly metastable due to diagenetic modifications (Moore, 2001; Lucia, 2007; Flügel, 2010). These challenges are a global issue, which motivated numerous researchers to study and document them to not remain relatively poorly understood, controversial, and far from being predictable (Al-Qayim et al., 2010; Swei and Tucker, 2012; Kolchugin et al., 2016, 2020; Lai et al., 2017, 2018; Zhu et al., 2020; Radwan et al., 2021; Liu et al., 2021; Wang et al., 2021; Abdel-Fattah et al., 2022; Abdullah et al., 2022; Boutaleb et al., 2022).

The Upper Devonian Dankovo-Lebedyansky sediments are considerable interest carbonates within the Volga-Ural Basin sequence because of their hydrocarbon reserves (Ibrahem et al., 2022a). Although Ibrahem et al. (2022a) provided important information on microfacies analysis and depositional environment of the Dankovo-Lebedyansky sediments in the studied area. There have been no studies performed on the impacts of microfacies and diagenesis on reservoir quality. However, understanding the depositional settings and microfacies, as well as the diagenetic modifications and their impacts on reservoir quality, is very important since the various microfacies have distinct petrophysical characteristics and can affect reservoir performance and hydrocarbon flow. Moreover, the diagenetic alterations (e.g., dolomitization, dissolution, and pressure dissolution) may produce high-quality reservoir rocks, making it a key issue in the oil exploration and development business from both academic and industrial perspectives.

This work is a detailed investigation of the Upper Devonian Dankovo-Lebedyansky sediments in three selected oilfields in Southeast Tatarstan (Fig. 1C and D) of the Volga-Ural Basin, focusing on impacts of microfacies and diagenesis on reservoir quality based on core investigations and thin section examinations combined with physical properties. Using an integrated approach through core analysis and well-log data, the present paper discussed and documented the following objectives: (i) A brief description of the Dankovo-Lebedyansky sediments' microfacies analyses and sedimentary facies belts. (ii) Recognize and document the diagenetic processes influencing the petrophysical properties of the Dankovo-Lebedyansky sediments. (iii) Porosity characterization and identification of a relationship between porosity and permeability, as well as microfacies and porosity. (iv) Define and document microfacies control on reservoir quality. (V) Identify and document the diagenetic process that controlled the petrophysical parameters of the Dankovo-Lebedyansky reservoir's quality. Understanding these objectives is crucial for a better understanding of reservoir properties in light of the present development activities of the studied fields as well as in nearby fields with similar settings.

2. Geological background

The Volga-Ural Basin (Fig. 1A, B and C) is a large Palaeozoic basin located on the Russian plain between the Volga River and the Ural Mountains to the west and the Peri-Caspian depression to the east and south (Ibrahem et al., 2022a, b). It is one of the oldest oil-producing basins in Russia, with the thickest sedimentary pile (Liang et al., 2015). It provided more than half of Russia's oil production until West Siberia surpassed it in 1978 (Kerimov et al., 2014). Many huge hydrocarbon fields, such as the supergiant Romashkino oil field (Fig. 1C) and the smaller adjacent fields, have been discovered in this basin.

The oilfields where the Dankovo-Lebedyansky sediments are studied and documented in this paper are located southeast of the

Tatarstan Republic, in Russia's eastern European part (Fig. 1C and D). From the Palaeozoic through the Cenozoic, carbonate and continental transitional clastic deposits accumulated in the Volga-Ural Basin (Fig. 2A) (Liang et al., 2020). Significant volumes of oil and gas have been discovered in the basin's terrigenous and carbonate reservoir layers (Fig. 2A), making it one of Russia's most productive hydrocarbon producers (Ibrahem et al., 2022a).

The primary hydrocarbon-producing formations in the Volga-Ural Basin are part of the Palaeozoic succession, which has a maximum thickness of about 1900 m (Liang et al., 2019). The reservoir interval of the Volga-Ural Basin lithostratigraphic section includes several Devonian and Carboniferous hydrocarbon-bearing units, as shown in Fig. 2A. The Upper Devonian (Frasnian-Lower Famennian) black shales are the source rocks. These units are composed of thinly bedded calcareous-siliceous successions containing abundant preserved organic matter (Galimov and Kamaleeva, 2015).

The studied interval in this paper covers the Middle Famennian of the Upper Devonian Dankovo-Lebedyansky sediments, which represent an interesting portion of the Volga-Ural Basin lithostratigraphic section and serve as a moderate-to-good hydrocarbon reservoir in several fields within the Tatarstan Republic territory (Ibrahem et al., 2022a).

Alexander Keyserling (1843) first identified the Dankovo-Lebedyansky sediments in the Volga-Ural petroleum province, and Strakhov (1939) named them (Strakhov, 1939). They were part of the Domanik-type formations, which stratigraphically extended from the Upper Devonian (Middle Frasnian) to the Lower Carboniferous (Tournaisian) (Liang et al., 2020). However, the Dankovo-Lebedyansky sediments are no longer considered part of the Domanik-type formations. This is due to variances in the sediment's lithological characteristics, where the Domanik-type formations consist of interbeds of limestone and siliceous carbonate rocks rich in organic matter and serve as both source and reservoir rocks (unconventional), while the Dankovo-Lebedyansky sediments consist of carbonates free of silica and serve only as reservoir rocks (Smirnov et al., 2018; Liang et al., 2020).

Within the Volga-Ural Basin, the Dankovo-Lebedyansky sediments (Fig. 2A and B) are conventional hydrocarbon sources. They are distinguished by large and cost-effective volumes of entrapped

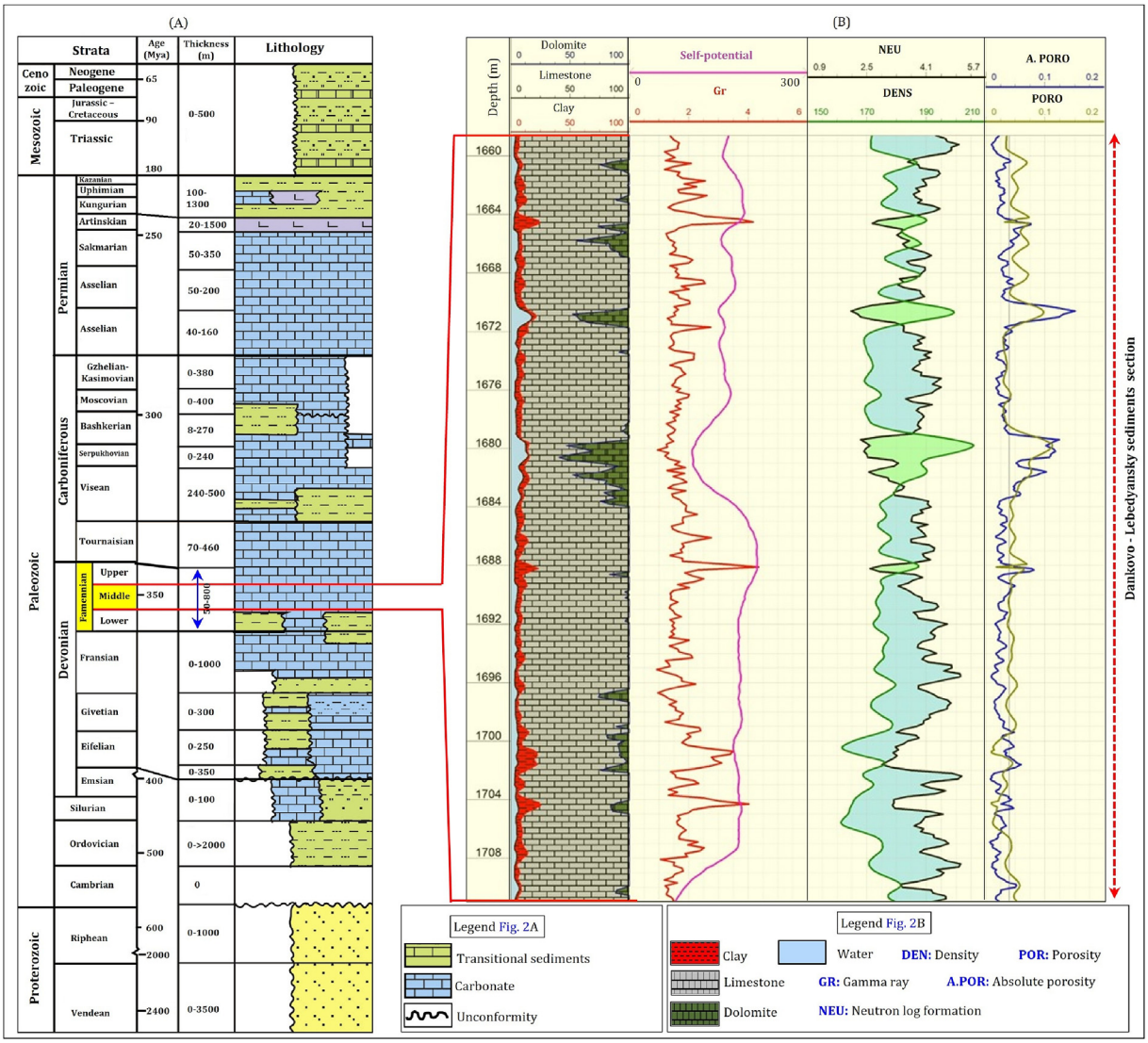

Fig. 2. (A) Generalized lithostratigraphy of the Volga-Ural petroleum province (Liang et al., 2020). The studied stratigraphical section (Middle Famennian of the Upper Devonian) is highlighted with a yellow color. (B) Dankovo-Lebedyansky lithological profile in the well X-3. The location of the well X-3 is shown in Fig. 1D. The first track in Fig. 1B presents depth in meter/measured depth (MD), and the second track presents the lithology log from petrophysical interpretations.

oil at depths ranging from 1300 to 1400 m (TVD). Dankovo-Lebedyansky sediments vary in thickness between 50 and 75 m, and productive zones vary in thickness between 3 and 10 m. Their sedimentary succession consists of limestone-rich marine carbonates interspersed with thin to medium-thick layers of secondary dolomites. The relationship between microfacies and diagenetic modifications is somewhat complicated, and it will be discussed further in the following sections.

3. Materials and methods

3.1. Materials

This study is based on data from four drilled oil wells referred to as X-1, X-2, X-3, and X-4 from three oilfields (Fig. 1D) that provided drilled cores containing up to 100 m of rock succession for laboratory analysis. For the petrographic analysis, almost 200 thin sections were cut from the core plugs. The selected samples represent the rock textures found in the carbonates of the Dankovo-Lebedyansky sediments according to the carbonate rock texture classification scheme proposed by Dunham (1962), as well as the porosity types according to the porosity classification schemes of the carbonates proposed by Choquette and Pray (1970), and Lucia (1995, 2007). The used wireline logs include lithology logs from petrophysical interpretations; lithology logs from core description; self-potential; gamma-ray (Gr); neutron log formation (NEU); density (DENS); absolute porosity (A. PORO); measured porosity (PORO); shallow and deep resistivity (IK and BK); calculated oil saturation (O-sat), calculated permeability (PERM), and zone index.

3.2. Methods

Flügel (2010) microfacies analysis approach is used to distinguish between the microfacies (MF) types and subdivide the sedimentary facies belts. By employing the sedimentological criteria, the carbonate classification scheme proposed by Dunham (1962) is used to classify the depositional texture types as well as microfacies. Cement classification schemes proposed by Folk (1959) and Longman (1980) were used for the petrographic subdivision of calcite and dolomite cements. To highlight the porosity, thin sections were impregnated with blue epoxy resin. The core slides were shot before being cut into thin sections to illustrate the rock's sedimentary texture.

The petrographic examinations of thin sections were performed using an optical polarizing microscope (Leica) in the lithology and mineralogy laboratory of the Institute of Geology and Petroleum Technologies at Kazan Federal University in order to perform microfacies analysis and investigate and document the sedimentary rock texture, size, and type of the grains, fossil types, identify the pore types, and characteristics of the diagenetic modifications, including types and distribution of the cements, etc. Thin sections were microphotographed with an optical polarizing microscope (Axio Imager A2), and Image-Pro Plus software was used to figure out the shape of the pores.

This study used the Core Laboratories CMSTM-300 system to measure the physical parameters of 100 plugs, including porosity and permeability. The porosity was measured using a helium porosimeter and computed using the pore volume and grain volume. The steady-state approach was used to calculate the horizontal permeability (Mukhametdinova et al., 2020). The reservoir can be divided into classes with distinct reservoir qualities by comparing the porosity and horizontal permeability data. Furthermore, the porosity values of the samples in each microfacies were compared with the dominant microfacies to highlight the microfacies with distinct reservoir characteristics. Petrel software was used to display the wells with their wireline logs and interpretations on a correlation panel. The oil saturation was calculated using statistical analysis and Techlog software.

4. Results

4.1. Microfacies

Ibrahem et al. (2022a) identified seven microfacies based on petrographic investigations and interpretations of the Dankovo-Lebedyansky sediment in the studied wells of the selected oilfields. These include peloidal grainstone MF 1, cemented bioclastic peloidal grainstone MF 2, echinoderm-concentrated packstone MF 3, algal packstone MF 4, bioclastic wackestone MF 5, whole-fossil wackestone MF 6, and dolomite MF 7. Table 1, and Fig. 3, illustrates the petrographic characteristics of each identified microfacies.

MF 1 consists of up to 85% of peloids that vary in size from 0.01 to 0.5 mm, spherical or ellipsoid in shape (Fig. 3A and B; abbreviated “Pel”). Between the peloids, patches of secondary calcite cement were observed (Fig. 3A and B; recognized by the white color on the thin section photomicrographs and abbreviated “Ca”, Table 1). MF 1 has well-developed primary intergranular and secondary leaching porosity, which thin-section examinations estimate to be up to 15% (Table 1).

MF 2 is characterized by a grain-supported peloidal texture with up to 30% calcite cement (Fig. 3C and D, Table 1). MF 2 lacks porosity due to the calcite fillings of the primary and secondary pores and reduces their sizes (Fig. 3D; indicated by the red circles).

MF 3 is characterized by a grain-supported texture with up to 20% micrites (Fig. 3E, Table 1). Crinoids are common (Fig. 3E; abbreviated “Echo”). Calcite accounts for up to 10% of MF 3 components and can be found surrounding the crinoids or in their chambers (Fig. 3E). Thin section examinations estimate up to 11% secondary porosity formed by the dissolution of stylolite, resulting in considerable channels (Fig. 3E).

MF 4 is distinguished by a high abundance of algae concentration (Fig. 3F; abbreviated “Alg”). Micrite accounts for up to 20% of MF 4 components, while calcite accounts for up to 10% (Table 1). Thin section examinations revealed that MF 4 has up to 12% porosity, which is mainly represented by secondary dissolution vugs and stylolites (Fig. 3F; abbreviated “Por”), while the syngenetic or primary pores are rare.

MF 5 is characterized by a micritic-supported texture with up to 60% of micrites (Fig. 3G, Table 1). 10%–30% of bioclast grains with sizes varying from 20 to 50 μm are presented. Calcite is common and accounts for up to 10% (Table 1), observed as fillings of the bioclast chambers and dissolution pores (Fig. 3G; abbreviated “Ca”). The overall porosity of MF 5 is not developed and thin section investigations estimate it to be up to 6%.

MF 6 is distinguished by micrite-supported texture, with more than 40% of micrites (Fig. 3H and I, Table 1). The grain-supported components are peloids or bioclasts such as ostracods (Fig. 3H; abbreviated “Ost”), calcispheres, and foraminifers. Calcite has been found to fill some pores and bioclasts, accounting for up to 10% of the total (Fig. 3H and I, Table 1). Thin section examinations estimate up to 6% porosity, which is not developed.

MF 7 consists of dolostone as a result of the host limestone dolomitization. Based on fabric and crystal features recognized by thin section examinations, six types of dolomites were identified in MF 7. Dolomitization and dolomite types go into detail in paragraph 4.3.2.2. Dolomite varies in crystal sizes between 10 μm and 200 μm and more. The secondary porosity of MF 7 is extensively developed and thin section investigations estimate it to be up to 16% (Table 1) consisting of vugular or intercrystalline pores.

Table 1
Microfacies codes, types, lithology, main components, estimated thin section porosity, and depositional environment of each microfacies type in the Dankovo-Lebedyansky sediments in the studied fields (modified after Ibrahem et al., 2022a).

Microfacies		Thin-section photograph	Main components	Carbonate grains			Cement		Estimated thin section porosity %	Dominant pore types	Depositional environment		
Code	Lithology			Peloids %	Intraclasts %	Bioclasts %	Calcite %	Micrite %					
MF 1	Peloidal grainstone	Fig. 3A and B	Peloids	85%	3%	5%	7%	5%	Good porosity up to 15%	The primary porosity is limited. The secondary porosity (vugs formed by leaching) is more common	Carbonate ramps	Inner ramp settings	Lagoon
MF 2	Cemented bioclastic peloidal grainstone	Fig. 3C and D	Peloids, bioclastic remains, and calcite cement	45%	5%	10%	30%	10%	Non or bad porosity, not more than 3%	The primary and secondary porosities are not developed			
MF 3	Echinoderm-concentrated packstone	Fig. 3E	Echinoderm with less micrite	30%	20%	20%	10%	20%	Good porosity up to 11%	The primary porosity is limited. The secondary porosity caused by dissolution or stylolite is well developed			Shoal
MF 4	Algae packstone	Fig. 3F	Algae with less micrite	30%	20%	20%	10%	20%	Good porosity up to 12%	The primary porosity is limited. The secondary porosity caused by dissolution or stylolite is well developed			
MF 5	Bioclastic wackestone	Fig. 3G	Bioclastic remains along with micrite	20%	5%	5%	10%	60%	Non or bad porosity, not more than 6%	The primary and secondary porosities are not developed		Middle and outer ramp settings	Open marine
MF 6	Whole-fossil wackestone	Fig. 3H and I	Bioclasts along with micrite	20%	5%	5%	10%	60%	Non or bad porosity, not more than 6%	The primary and secondary porosities are not developed			
MF 7	Dolostone	Fig. 6	Dolomite	5%	0%	1%	2%	5%	Good porosity up to 16%	The secondary inter-crystalline pores are well developed			

4.2. Sedimentary facies belts and depositional model

Using Flügel (2010) classification, the identified microfacies were grouped into facies associations based on their characteristics and depositional settings. Fig. 4A and B illustrate the facies association belts of the Dankovo-Lebedyansky sediments, which include lagoon, shoal, and open marine settings within a general carbonate ramp environment (inner, middle, and outer ramp) (Ibrahem et al., 2022a). The characteristics of each facies' associations are discussed in the following paragraphs.

4.2.1. The inner ramp settings

Thin section petrography examinations (Fig. 3) revealed that MF 1, MF 2, MF 3, and MF 4 were deposited in inner ramp settings (Ibrahem et al., 2022a). MF 1 has the minimum amount of micritic matrix (Table 1) as well as various sizes of peloids and intraclasts that are surrounded by secondary calcite cements in the form of rims around the grains (Fig. 3A and B); this suggests that MF 1 was deposited in an inner ramp characterized by high to moderate energy depositional conditions (Flügel, 2010). MF 2 (Fig. 3C and D) is also thought to have formed within an inner ramp environment (Fig. 4A and B). This interpretation is supported by the tangential to radial intensive of the calcite cementation, which suggests high to moderate depositional energy (Flügel, 2010). MF 3 (Fig. 3E) and MF 4 (Fig. 3F) show relatively good preservation degrees of the echinoderm and algae skeleton. According to Flügel (2010), this indicates that they were either already at the deposition site or were transported a short distance before deposition.

4.2.2. The middle and outer ramp settings

Thin section petrography examinations (Fig. 3) show that MF 5 and MF 6 were deposited in the middle ramp settings. The presence of mud components (Fig. 3G, H, and I, Table 1), grain micritization, the moderate degrees of sorting, as well as the common presence of open marine bioclasts such as bivalves, gastropods, calcispheres, and foraminifers, points to the middle and outer ramps (Fig. 4A and B), with relatively deeper water depth and moderate sedimentation rates (Tucker and Wright, 1990).

4.3. Diagenetic characteristics

Once sediments are deposited in the sedimentary basin, they undergo diagenesis, which is a series of processes that alter the physical, chemical, or mineralogical properties of the host rocks, resulting in more stable components (Noel and Brian, 2015). The Dankovo-Lebedyansky sediment reservoir characteristics are a consequence of the depositional settings and diagenetic modifications to the initial sedimentary texture. Thin section petrographic examinations enabled identification of the main diagenetic events and their characteristics that impacted the Dankovo-Lebedyansky sediments. These include micritization, calcite cementation, dolomitization, dissolution, compaction, and microfracturing, which are further detailed below with the goal of clarifying the link between microfacies and diagenetic alterations and their impact on reservoir quality.

4.3.1. Micritization

Thin section examinations confirmed the presence of micritization features in many of the examined samples (Fig. 5). They may be difficult to distinguish from the surrounding fine-grained micritic matrix. Completely micritized skeletal grains (peloids) are widespread and observed in almost all the recognized

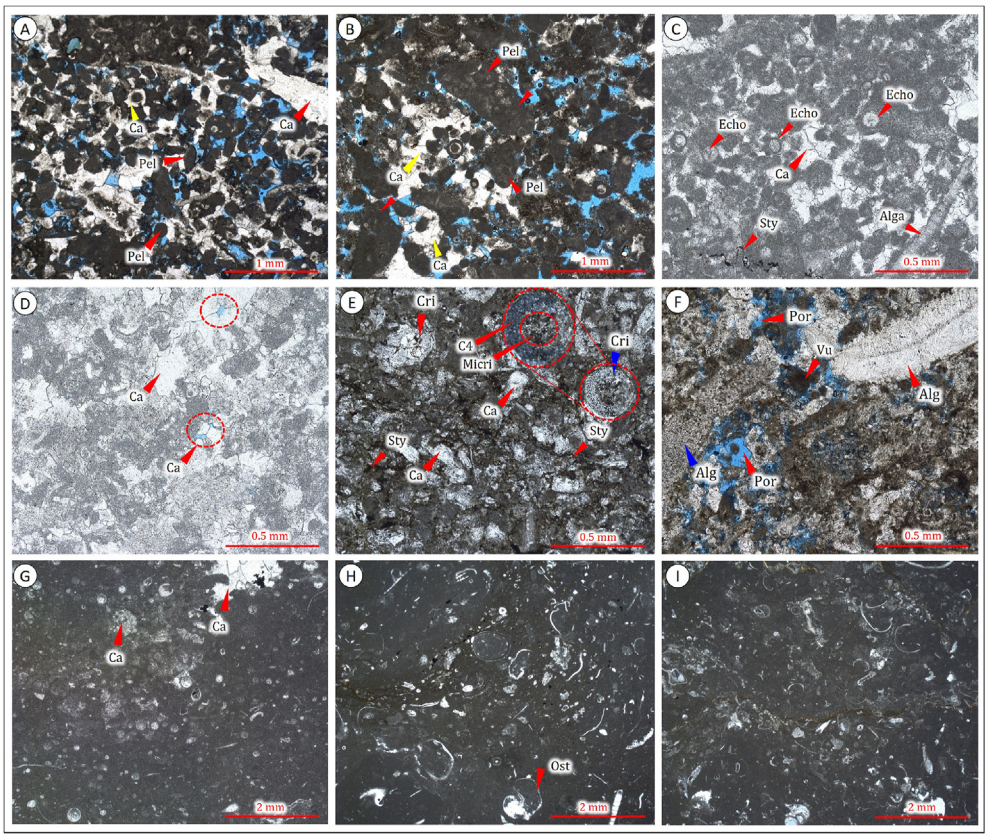

Fig. 3. Representative plane-polarized light (PPL) thin section photomicrographs of the identified microfacies types in the Dankovo-Lebedyansky sediments show: (A, B) Peloidal grainstone MF 1, peloids vary in size from 0.01 to 0.5 mm, dissolution pores are common, secondary calcite fills some pores or surrounds the peloids. (C, D) Cemented bioclastic peloidal grainstone MF 2, bioclasts up to 2 mm in size, micro-sparry calcite aggregates filling the pore spaces. (E) Echinoderm-concentrated packstone MF 3, crinoids are prevalent, stylolite is also present, secondary micro-sparry calcite fills some of the crinoids' internal structure. (F) Algae packstone MF 4, algal fragments up to 1 mm in size intermixed in with smaller foraminifera, common vuggy pores up to 0.1 mm in size. (G) Bioclastic wackestone MF 5, calcisphere, and ostracod inclusions are presented, micro-sparry calcite aggregates are also presented. (H, I) Whole-fossil wackestone MF 6, ostracod and calcisphere shell inclusions are abundant, stylolite is uncommon. Abbreviations: Pel - Peloids; Ca - Calcite; Echo - Echinoderm; Alg - algae; Sty - Stylolite; Cri - Crinoid; Por - Pores; Vu - Vugs; Ost - Ostracod.

microfacies, although they are most prominent in MF 1 and MF 2. Micritization created micritic rims or envelopes of a few micrometers enclosing or coating the outer margins of the skeletal grains, as shown in Fig. 5A and B; the micritic rims are marked by the red arrows and abbreviated “Micri”. Micritization also occurs as an entire or partial replacement of the interior structures of the algae skeletal grains by micrite (Fig. 5C; abbreviated “Micri").

4.3.2. Cementation

Cementation is the primary pore-destructive diagenesis (Moore, 2001; Flügel, 2010). When sediments undergo diagenetic processes, chemical precipitates in the form of new crystals within the pore spaces bond or cement the grains (Tucker, 2001). Thin section examinations revealed that the most prevalent cementing materials observed in the Dankovo-Lebedyansky sediments are calcite and dolomite. They are discussed more below.

4.3.2.1. Calcite cement. Calcite is the most common type of cement. Based on fabric and crystal characteristics (Folk, 1965; Longman, 1980), it is subdivided into six types: isopachous rim calcite C1, bladed rim calcite C2, drusy calcite C3, syntaxial calcite C4, drusy pore-filling calcite C5, and granular fracture-filling calcite C6. Each type is described below.

Isopachous rim calcite C1: This type of calcite cement is the most prevalent in MF 1 and MF 2, although it is less common in the other microfacies. It was observed as thin as 10 μm thick rims, coating the outer margins of the non-skeletal peloid grains (Fig. 5D; abbreviated “C1″) or skeletal grains (Fig. 5 E; abbreviated “C1″), or as bundles composed of very fine to fine-medium calcite crystals buried within the micritic groundmass and varying in size from 10 μm to 100 μm, rarely exceeding 200 μm, partially or totally occluding the primary and secondary pores (Fig. 5D and E; abbreviated “C1″).

Bladed rim calcite C2: It is the most common calcite cement type in MF 1 and MF 2 and is characterized by its growth surrounding the peloids grains and forming rims or coatings of up to 20 μm thick, as well as filling or lining the interparticle pores, significantly reducing their diameters and partially or totally occluding them (Fig. 5F; abbreviated “C2″). C2 calcite can be wider than C1 calcite, with crystal lengths exceeding 200 μm as shown in Fig. 5F due to the development of C2 calcite over C1 calcite, particularly when the pore spaces are open and don't contain any secondary mineralization that could inhibit the calcite crystals growth (Folk, 1965; Zhu et al., 2020).

Drusy calcite C3: C3 calcite is the dominating calcite cement in MF 1. It was observed as filling cement in the interparticle or intraparticle pores (Fig. 5F; abbreviated “C3″). It might be developed over C1 or C2 calcite cements in the pore spaces or around the grains. C3 calcite cement crystals grow gradually towards the pore spaces center, reducing their diameters or totally blocking them (Fig. 5F).

Syntaxial calcite C4: This type of calcite is common in MF 3 and

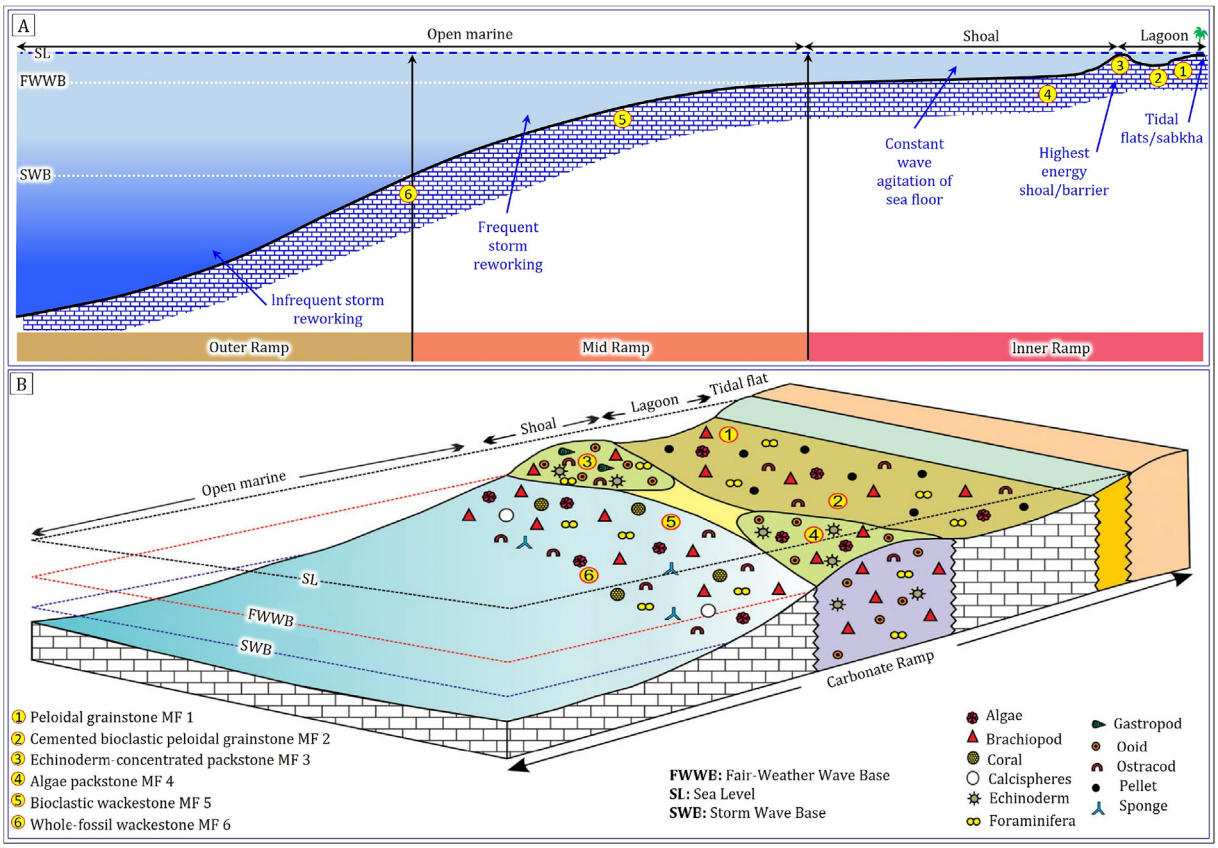

Fig. 4. General depositional model for the Upper Devonian Dankovo-Lebedyansky sediments in the studied fields based on microfacies analysis. (A) The depositional profile extends from the lagoon-shoal to the open marine with the locations of the deposited microfacies. (B) Distribution and abundance of microfacies belts in the carbonate ramp depositional environments along with microfacies components (Ahmad et al., 2021; Ibrahem et al., 2022a).

MF 4. It consists of fine crystals that fill the inner pore structure of echinoderms (see Fig. 3E; indicated by the red circle). Here, calcite crystal growth rapidly decreases towards the centers of the echinoderms due to their filling with micrite. C4 calcite was also observed as developed crystals growing within pore spaces, particularly those that are open and characterized by the availability of spaces and the absence of secondary mineralization, which did not restrict calcite crystal growth (Fig. 5F; abbreviated "C4″). C4 calcite crystals may grow and expand over the earlier formed calcite cement crystals (C1, C2, and C3), postdating their development, coating the pore spaces, and decreasing their interdiameters (Fig. 5F). Furthermore, C4 calcite cement, observed as fillings of pore spaces created by the skeletal or non-skeletal grains' dissolution (Fig. 5G). Here, it is composed of calcite crystals varying in size from fine (Fig. 5G; indicated by the red arrow and abbreviated "C4″) to coarse, even poikilotopic, monocrystal overgrowth crystals that almost occlude the interior pore space (Fig. 5G; indicated by the yellow arrow and abbreviated "C4″). C4 calcite cement can also be found in the form of thin, 10 μm-diameter calcite rims coating the inner margins of dissolved grains (Fig. 5G; indicated by the blue arrow and abbreviated "C4″).

Drusy pore-filling calcite C5: This type of calcite cement is common in MF 2 and MF 5. It is composed of fine 30 μm or drusy up to 100 μm calcite crystals that fill the moldic or interparticle pores (Fig. 5H; abbreviated "C5″). The growth of C5 calcite crystals within the pore spaces causes them to develop over the other calcite crystals, resulting in reducing the pore diameters or occluding them (Fig. 5H; abbreviated "C5″).

Granular fracture-filling calcite C6: This calcite type is common in MF 2 and MF 5. It was observed in the form of calcite patches consisting of subhedral to anhedral crystals that fill the microfracture spaces (Fig. 5I; abbreviated "C6″). The C6 calcite most likely developed over other types of calcite cement, resulting in the crystal growth and total occlusion of the pore spaces that occupy them (Fig. 5I; abbreviated "C6″).

4.3.2.2. Dolomitization and dolomite cement. Based on the macroscopical investigations of the cored intervals (Fig. 6) and well log interpretation (see Fig. 2B), dolomite intervals with thicknesses varying from 50 cm to 4 m were identified in the Dankovo-Lebedyansky sediment section. When the cavities are saturated with residual oil, the resulting dolomite has a blackish color and a brittle texture (Fig. 6A), while when the cavities are empty, the dolomite has a grey-green color and a dense texture (Fig. 6D). Petrography thin section examination identified six types of dolomites based on fabric and crystal properties proposed by Folk (1965) and Longman (1980). Each type of the identified dolomites is described below.

D1 dolomite/dolowackestone: The selective D1 dolomite is frequently encountered as a replacement of the host limestone in MF 5 and MF 6. It has a fine crystalline structure with crystals as very fine as 10 μm in size (Fig. 6B and C, abbreviated "D1″). D1 dolomite is observed as a replacement of the micritic matrix associated along the microfracture pathway (Fig. 6B and C; indicated by MF-Zone). This suggests that it served as a dolomitization fluid pathway (Sibley and Gregg, 1987).

D2 dolomite/fine crystalline planar-s: The D2 dolomite has a fine crystalline texture with crystals varying in size between 10 μm and

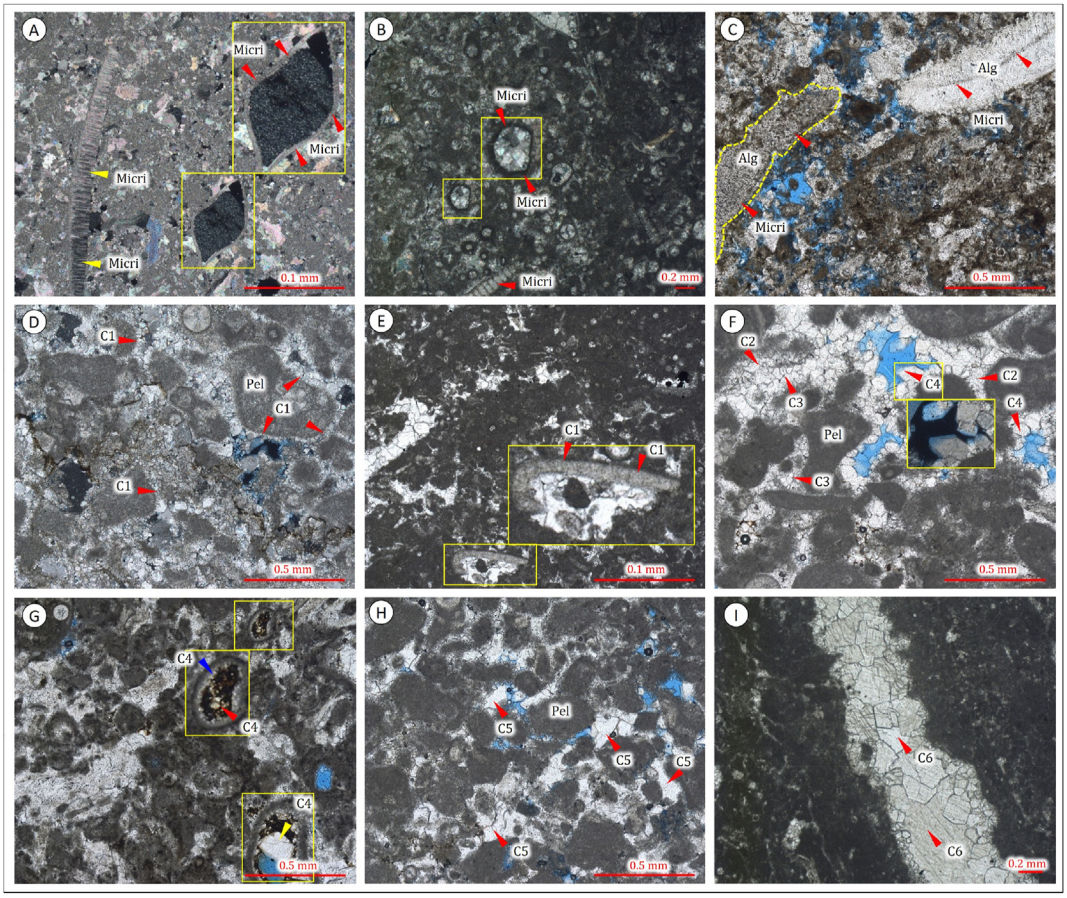

Fig. 5. Representative plane-polarized light (PPL) thin section photomicrographs of the Dankovo-Lebedyansky sediments showing: (A and B) Peloidal packstone MF 1 with micritization features abbreviated "Micri," micritic rimes surrounding the bioclasts or within their inner chambers. (C) Algae packstone with micritized algae fragments. (D) Peloidal grainstone with common C1 calcite cement buried within the matrix and surrounding the peloids. (E) Cemented bioclastic peloidal grainstone with common C1 calcite as coatings around the bioclasts. (F) Peloidal grainstone with common C2, C3, and C4 calcites forms rims or coatings surrounding the grains and filling the interparticle pores. (G) Peloidal packstone with common C4 calcite cement fills or lines the vugs caused by dissolution. (H) Peloidal grainstone with common C5 calcite cement as interparticle pore fillings. (I) Patches of subhedral to anhedral crystals of C6 calcite fill the microfracture spaces. Abbreviations: Micri - Micritization; C1 – C1 calcite cement; C2 – C2 calcite cement; C3 – C3 calcite cement; C4 – C4 calcite cement; C5 – C5 calcite cement; C6 – C6 calcite cement; Pel - Peloids; Alg - algae.

20 μm and a planar-s crystalline structure (Fig. 6E). Typically, D2 dolomite comprises a homogeneous ground mass with grey irregular clouds or ghosts of the original micritic grains (Fig. 6E; abbreviated "Mic"). Dolomite crystals are anhedral in shape, particularly when they are of a fine crystalline texture up to 10 μm in size, with no relics of the original fabric except for remnants of the original micritic grains (Fig. 6E; abbreviated "Mic"), which were not subjected to the dolomitization process (Boutaleb et al., 2022; Zhu et al., 2020). D2 dolomite displays an abundance of moldic to vugular porosity (Fig. 6E, abbreviated "Por").

D3 dolomite/medium crystalline planar-e-s: The D3 dolomite has a medium crystalline texture with crystals varying in size from 20 μm to 50 μm, and even coarsely up to 100 μm (Fig. 6F). The common crystalline type of D3 dolomite is planar-e-s (Sibley and Gregg, 1987). Thin section photomicrographs show that the texture of D3 dolomite has remains of the original micritic grains (Fig. 6F; areas indicated by the red circles). The most common type of porosity in D3 dolomites is intercrystalline porosity (Fig. 6F; abbreviated "Por"), which often increases in the coarser crystalline fabric and coalesces to form isolated vugs (Fig. 6F, indicated by the yellow arrows and abbreviated "Por").

D4 dolomite/coarse crystalline planar-e-s: D4 dolomite has a coarse crystalline structure with crystal sizes varying from 50 m to 100 m or larger (Fig. 6G). The most common porosities are intercrystalline and vuggy (Fig. 6G; abbreviated "Por"). The original micritic matrix has been noticed in the dolomite crystals' cloudy centers (Fig. 6G; abbreviated "Mic"). The D4 dolomite crystals are quite coarse and show dissolving gradually (Fig. 6G; areas indicated by the red circles and abbreviated "Por").

D5 dolomite/dolomite cement planar-e-s: D5 dolomite has a patchy crystal distribution with sizes varying from 50 μm to 500 μm and a clean, homogeneous, spotty, coarse to extremely coarse crystalline structure (Fig. 6H). Gregg and Sibley's (1984) saddle dolomites are identical to the D5 dolomite. Thin section photomicrographs exhibit several halos from the original micrite (Fig. 6H, abbreviated "Mic"). D5 dolomite has the texture of dedolomitized dolomite as a result of repeated dolomite replacement and cementation (Sibley, 1982; Al-Qayim et al., 2010). Excessive dolomite crystal formation causes pore space obstruction (Fig. 6H, areas indicated by the red circles and abbreviated "Por").

D6 dolomite/bimodal: The D6 dolomite differs from the other dolomite types by having a mixture of dolomite crystal sizes (Longman, 1980; Al-Qayim et al., 2010). It is composed of fine and medium crystalline mosaic (Fig. 6I) or coarse and medium crystalline mosaic (Fig. 6I); in both examples, the finer fractions have an anhedral to subhedral crystal structure, while the coarsest fractions are typically euhedral.

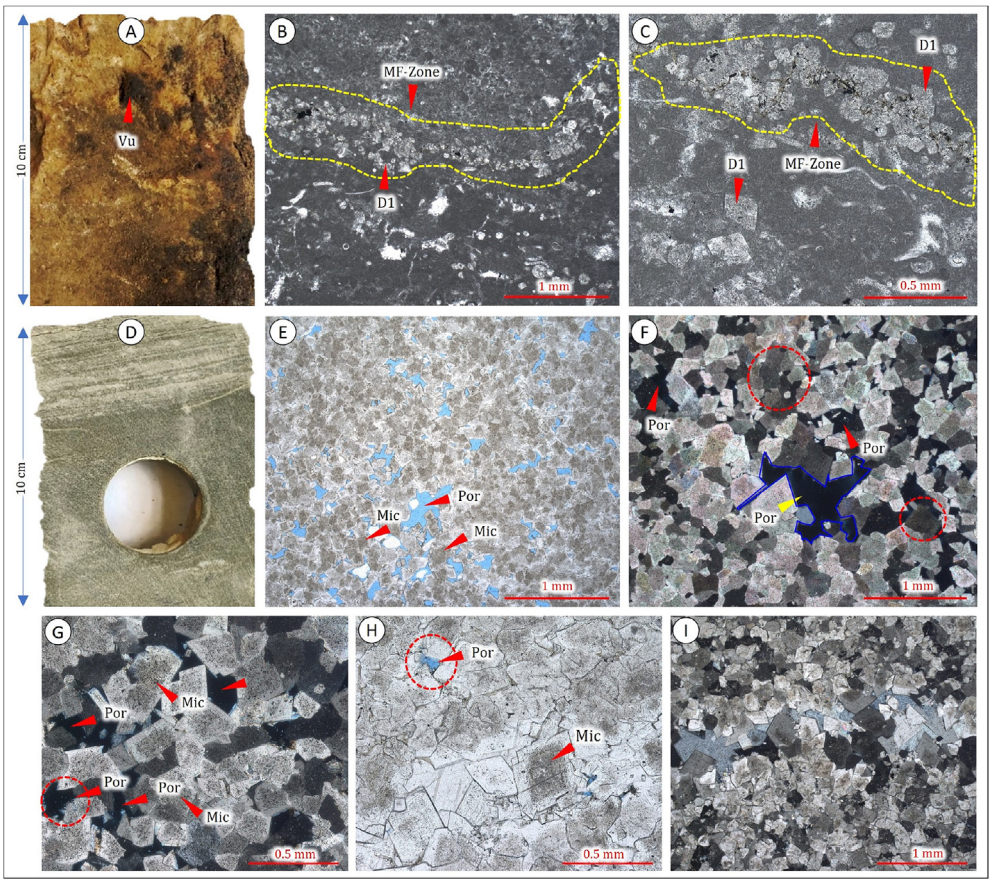

Fig. 6. Representative core photographs taken in natural light and plane-polarized light (PPL) thin section photomicrographs of the Dankovo-Lebedyansky sediments showing: (A) Dolomite, dark brown, unevenly saturated with oil, brittle texture, visible vugs. (B, C) Bioclastic wackestone MF 5 with common D1 dolomite as a replacement of the micritic matrix or along the microfracture pathway. (D) Dolomite, grey-green, calcareous, with a dense texture. (E) Fine crystalline D2 dolomite, remnants of the original micritic abbreviated "Mic", abundance of moldic to vugular porosity abbreviated "Por". (F) Medium crystalline D3 dolomite. Remnants of the original micritic are indicated by the red circles. Intercrystalline and vug porosities are common. (G) Coarse crystalline D4 dolomite, with prevalent intercrystalline and vuggy porosities, remnants of the original micritic matrix, abbreviated "Mic". (H) D5 dolomite, the remnant pores are closed due to the excessive growth of dolomite crystals. (I) Bimodal D6 dolomite consists of a mixed form of dolomite crystal sizes. Abbreviations: Vu - Vugs; MF-Zone - Microfracture zone; D1 - D1 dolomite; Por - Pores; Mic - Micrite.

4.3.3. Dissolution

Dissolution refers to the dissolving processes of the skeletal or non-skeletal components that occur in the carbonate rock texture as a result of their interaction with fresh or saltwater. It is the primary process that produces a variety of distinct textures and contributes to the quality development of the reservoir layers by forming secondary moldic and vuggy pores, particularly when secondary mineralization within the pore network is lacking (Moore, 2001; Lucia, 2007; Flügel, 2010).

The macroscopical investigations of the cored intervals, as well as microscopical petrographic examinations of the thin sections from the Dankovo-Lebedyansky sediments (Fig. 7), revealed that multiple fabric-selective and non-fabric-selective dissolution events occurred to variable degrees practically in all of the identified microfacies.

Dissolution is more common in the microfacies with coarser granular components, such as peloidal grainstone MF 1 (Fig. 7B and C), echinoderm-concentrated packstone MF 3 (Fig. 7E), and algae packstone MF 4 (Fig. 7F), whereas it is less common or non-existent in the microfacies with finer components, such as cemented bioclastic peloidal grainstone MF 2, bioclastic wackestone MF 5 (Fig. 7H and I), and whole-fossil wackestone MF 6. Ehrenberg et al. (2012) proposed that this is because the mudstone and wackestone microfacies, which consist of finer granular components, did not have enough channels or primary intergranular porosity during the early diagenesis to allow dissolution fluids to pass through. On the other hand, packstone and grainstone microfacies, which consist of coarser granular components, have higher primary porosity.

The fabric-selective dissolution of MF 1's peloids and unstable bioclasts increases the secondary porosity by forming moldic pores and vugs that can be isolated or poorly connected, inhibiting fluid flow, or well connected, facilitating fluid flow (Fig. 7B and C; indicated by the blue areas in the thin section photomicrographs and by the red arrows).

Non-fabric-selective dissolution is also common in porous microfacies like MF 1 (Fig. 7B and C), MF 3 (Fig. 7E), and MF 4 (Fig. 7F). This type of dissolution results in the formation of secondary porosity, which is represented by channels and cavities that pass through the rock components such as the non-skeletal or skeletal grains, micritic matrix, or the previously formed cement, in addition to stylolites, which may occasionally be enlarged due to the dissolution activities, thereby improving reservoir quality (Fig. 7E; indicated by the forked lines in the thin section photomicrography).

Fabric-selective and non-fabric-selective dissolution processes have also been observed in the finer-component microfacies such as MF 2, MF 5, and MF 6. It dissolves some of the micritic matrix or earlier formed cement and may, in exceptional cases, have an

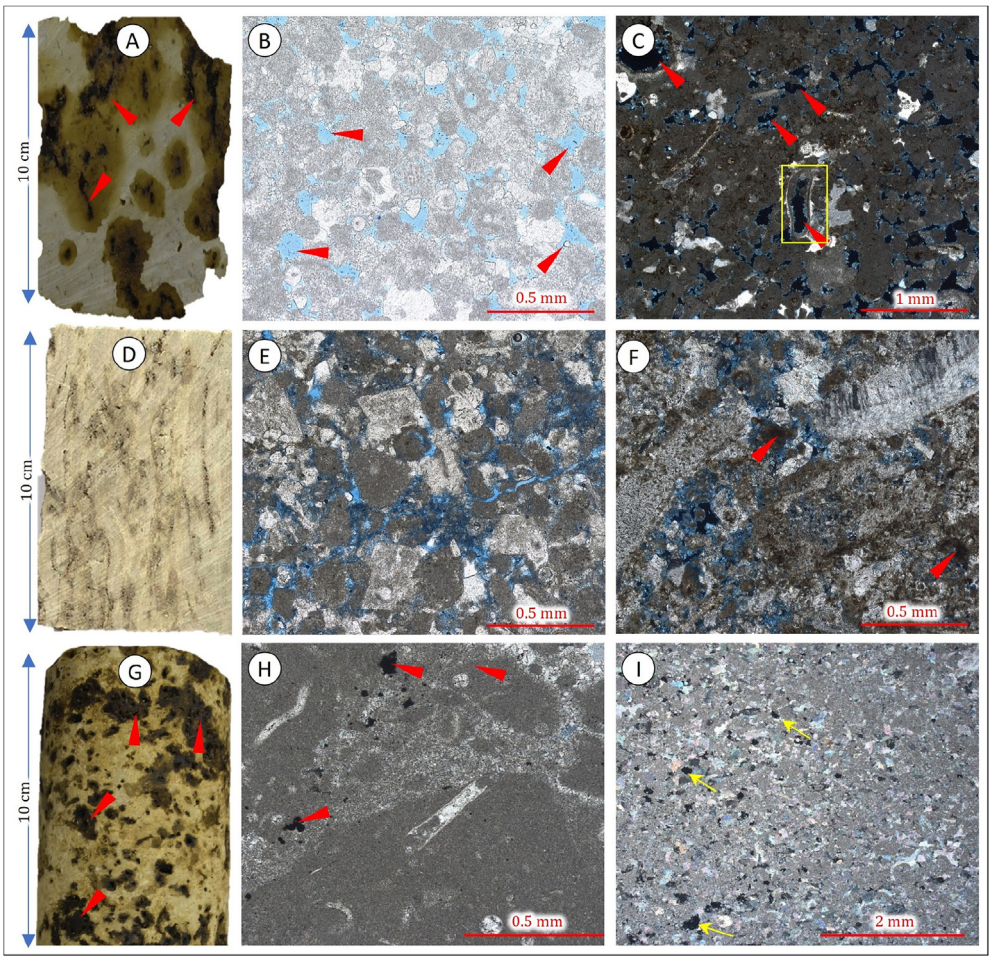

Fig. 7. Representative core photographs taken in natural light and plane-polarized light (PPL) thin section photomicrographs of the Dankovo-Lebedyansky sediments showing: (A) Well-developed dissolving vugs with diameters of more than 1 mm that are filled with residual hydrocarbons (indicated by the red arrows). (B) Peloidal grainstone MF 1, vugs are extensively formed and interconnected due to the dissolution of peloids (indicated by red arrows). (C) Peloidal grainstone MF 1, vugs are well developed as a result of the skeletal grains' dissolution (shown by the red arrows). Secondary calcite precipitates along the inner edges of the pores. (D) Well-developed vugs and stylolites that have been enlarged by dissolution. (E) Echinoderm-concentrated packstone MF 3, vugs and stylolites with diameters of 0.5–1 mm or more enlarged by dissolution, pores are well connected. (F) Algae packstone MF 4 with formed vugs due to dissolution, vugs containing residual hydrocarbons (indicated by red arrows). (G) Well-developed vugs with widths of more than 1 mm (indicated by the red arrows), filled with residual hydrocarbons. (H, I) Bioclastic wackestone with undeveloped vugs due to dissolution of some parts of the micritic matrix (indicated by the yellow arrows).

influence on the finer bioclasts (Fig. 7H and K). These dissolution events result in secondary porosity, which is seen as vugs of varying diameters. However, since MF 2, MF 5, and MF 6 lack reservoir properties like porosity and permeability, these vugs do not contribute to improving the reservoir quality of these microfacies sediments.

4.3.4. Compaction

Compaction is the process of reducing the bulk volume of rocks; it is controlled by several factors, including sedimentary load, temperature, and sediment pressure during burial, as well as pore pressure and pore fluid chemical composition (Moore, 2001). Compaction involves both mechanical and chemical compaction (Tucker, 2001). Mechanical compaction is often more noticeable in coarser granular microfacies than in finer ones. In other words, when transferring from grainstone or wackestone to mudstone, mechanical compaction is more obvious (Tucker, 2001). This might be explained by the fact that the micritic cement surrounding and between the grains is more resistant to compaction due to the small size of its components.

Mechanical compaction is represented in the Dankovo-Lebedyansky sediments by i) Multiple fragments of shattered grains, compressing or deforming the enclosed bioclasts (Fig. 8A; indicated by the red arrow). The lack of cement between the grains assists in the development of mechanical compaction processes (Flügel, 2010). ii) Reorientation of the rock texture, including skeletal and non-skeletal components, in line with the compaction direction (Fig. 8B; indicated by the yellow zone). iii) Due to their muddy nature, the smaller-sized peloids have notable mechanical compaction effects that assist in responding to the compaction (Fig. 8C; indicated by the yellow arrows).

Chemical compaction refers to processes that occur later in diagenesis as a result of overburden and tectonic compaction (Tucker, 2001). The effects of chemical compaction in the Dankovo-Lebedyansky sediments are represented by: i) presence of the stylolites or dissolution seams (Fig. 8D and E; indicated by the red arrows and abbreviated “Sty”) that formed as a result of the overburden, where grain-to-grain interactions first occurred and then grew into planar and sutured grain contacts, resulting in the formation of stylolites (Bjørlykke, 2014). In the majority of the

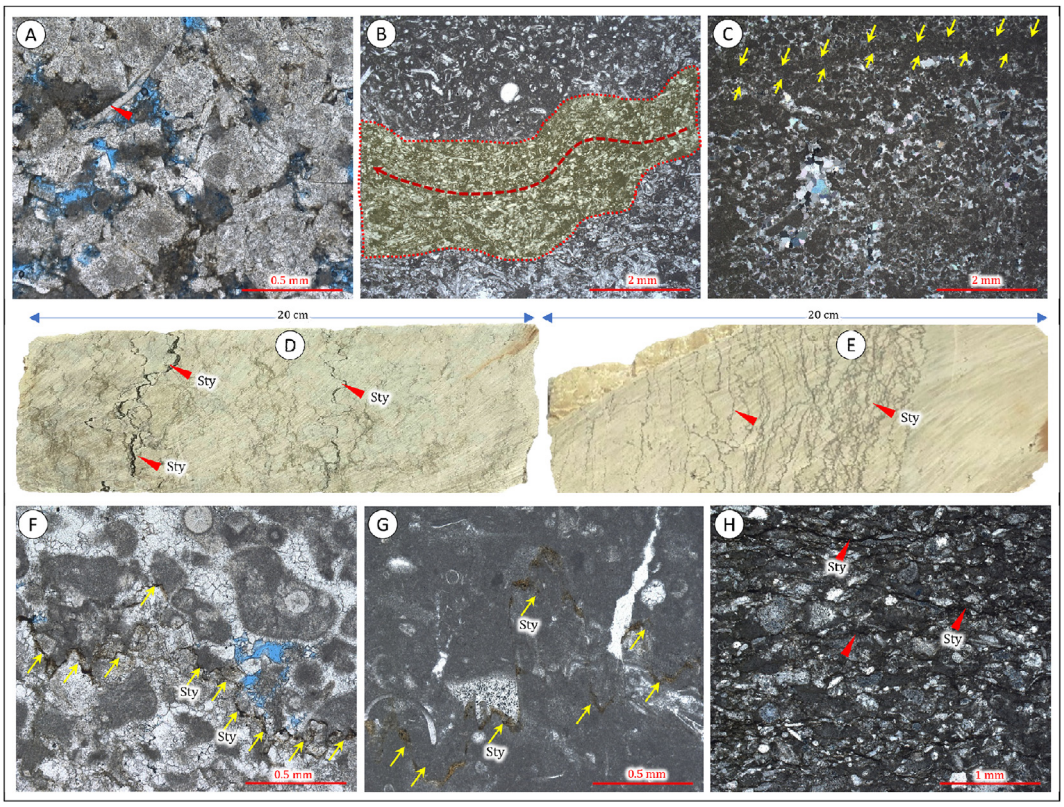

Fig. 8. Representative core photographs taken in natural light and plane-polarized light (PPL) thin section photomicrographs of the Dankovo-Lebedyansky sediments showing: (A) Peloidal grainstone MF 1 with shattered grains into multiple fragments under the effects of mechanical compaction. Bioclasts are also influenced by compaction (indicated by the red arrow). (B, C) Compaction and reorientation of the rock components under the effects of mechanical compaction (indicated by the yellow zone). (D and E) Compaction features in the Dankovo-Lebedyansky sediments. (F) Peloidal grainstone MF 1 with stylolite microfracture (indicated by the yellow arrows). (G) Stylolite "Sty" is a result of chemical compaction (indicated by the yellow arrows). (H) Dissolution channels as a result of chemical compaction in the form of capillary channels with micrometer widths across the micritic matrix.

examined samples, insoluble remnants of dark-colored organic debris or bituminous concentrates were observed along the stylolites (Fig. 8F and G). ii) Chemical compaction causes the formation of dissolution channels that cross the matrix in the form of capillary channels with diameters of a few micrometers (Fig. 8H; indicated by the red arrows). Stylolites are more prevalent in MF 1, MF 3, and MF 4, but less prevalent in MF 2, MF 5, and MF 6. This is explained by the extensive cementation of these microfacies components with calcite cement or due to their muddy nature, which precluded the stylolite formation (Bjørlykke, 2014). Pressure dissolution might be a major source of CaCO3 for burial cementation (Flügel, 2004; Bjørlykke, 2014).

4.3.5. Microfractures

The presence of microfractures in the Dankovo-Lebedyansky sediments is unusual. Some microfractures up to 5 mm wide and filled with calcite have been observed (see Fig. 5J). Other evidence can be found in some intervals that have been dolomitized (see Fig. 6B and C). They are partially filled with dolomite.

4.4. Porosity characterization

The porosity values obtained from the core-plug analysis vary between 1% and 17% (mean = 6.8%), while the permeability values vary between 0.05 mD and 100 mD (mean = 70 mD). The cross plot (Fig. 9A) shows a substantial relationship between the porosity and permeability values and microfacies types. The high porosity and permeability values correlate to MF 1 (max 16.5%), MF 3 (max 14%), MF 4 (max 13%), and MF 7 (max 17%). On the other hand, the low porosity and permeability values correspond to MF 2 (max 5%), MF 5 (max 7.5%), and MF 6 (max 8.5%).

Furthermore, as shown in Fig. 9B, the estimated porosity values obtained by thin section examination vary between 0.6 and 16% (mean = 6.13%) for all samples of the identified microfacies. Despite the presence of some points in the dolomite MF 7, as indicated by the blue arrow, which is typical for samples dominated by dolomite cement, which blocks the pore spaces, as shown in Fig. 6H and I, the histogram in Fig. 9B demonstrate a significant correlation between the microfacies type and porosity values.

The porosity values in Fig. 9B vary significantly depending on the microfacies type. MF 1 has the highest porosity values, up to 16%, followed by MF 3 and MF 4, with porosity values of up to 12%. The dolomite MF 7 is further distinguished by high porosity values of up to 16%. In contrast, MF 2, MF 5, and MF 6 have the lowest porosity values (max 6%).

Fig. 10 illustrates a correlation panel of the Dankovo-Lebedyansky sediments between the studied wells. MF 1, MF 3, MF 4, and MF 7 correspond to reservoir units with the highest porosity and oil saturation. Non-reservoir units with the lowest porosity and oil saturation correspond to MF 2, MF 5, and MF 6.

5. Discussion

5.1. Diagenetic history

Based on petrographic results and relationships between the

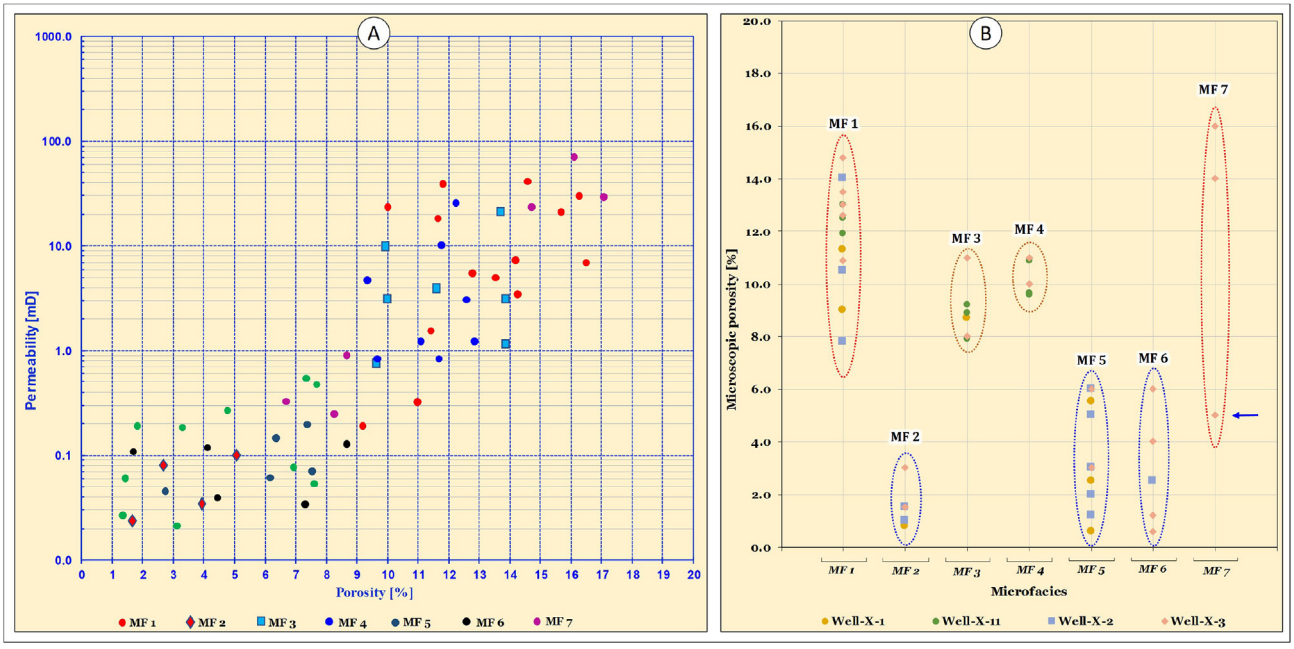

Fig. 9. (A) Cross-plot showing the correlation between the core-derived porosity and permeability values with microfacies types of the Dankovo - Lebedyansky sediments section in the studied wells. (B) Representative cross-plot showing the correlation between thin sections-estimated porosity values with microfacies types of the Dankovo - Lebedyansky sediments section in the studied wells (the blue arrow indicates some outliers in the dolomite microfacies MF 7). The locations of the studied wells are shown in Fig. 1D. Porosity values are in percent (%), while permeability values are in millidarcy (mD). MF 1: peloidal grainstone, MF 2: cemented bioclastic peloidal grainstone, MF 3: echinoderm-concentrated packstone, MF 4: algae packstone, MF 5: bioclastic wackestone, MF6: whole-fossil wackestone, and MF7: dolomites.

various diagenetic events identified by thin section petrographic examinations, as well as interpretations from the literature (; Al-Qayim et al., 2010; Kolchugin et al., 2016, 2020; Smirnov et al., 2018; Zhu et al., 2020; Liu et al., 2021; Wang et al., 2021). The relative timing and history of the diagenetic events documented in the Dankovo-Lebedyansky sediments were reconstructed, taking into account that the sediments' present depth to the base is up to 1800 m (measured depth). As indicated in Fig. 11, diagenesis of the Dankovo-Lebedyansky deposits is suggested to have occurred in the marine-meteoric mixing zone, the shallow burial, and the

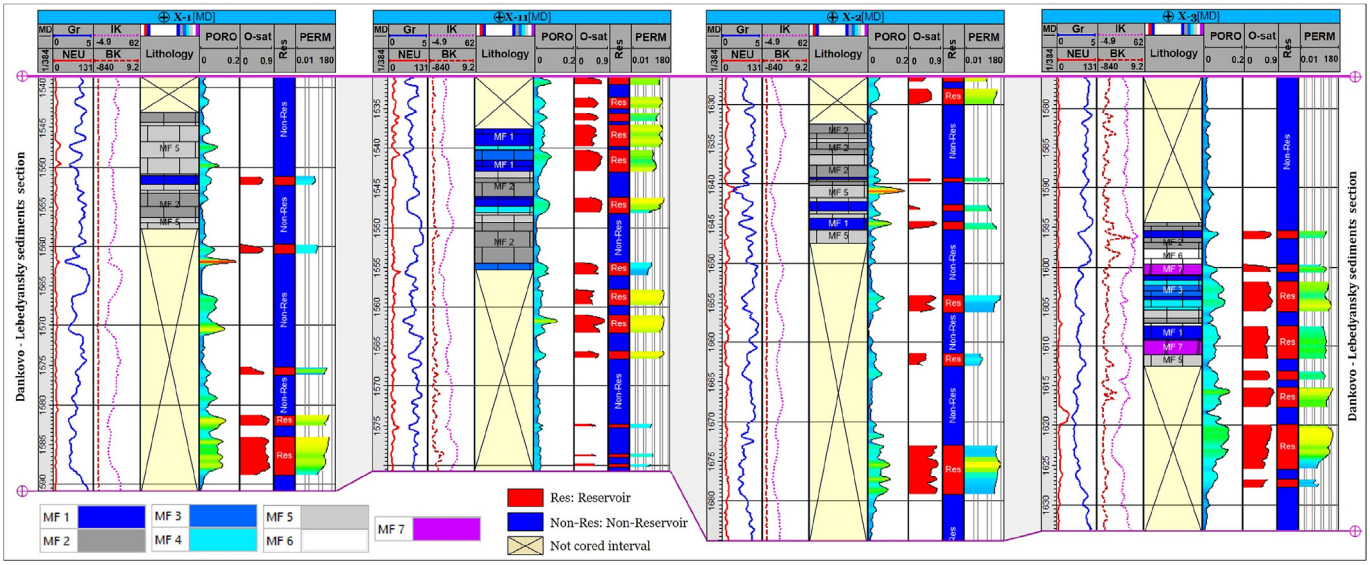

Fig. 10. (A) Representative correlation panel of the Dankovo - Lebedyansky sediments section in the studied wells. The locations of the studied wells are shown in Fig. 1D. Measured porosity (PORO) values are in percent (%). Calculated oil saturation (O-sat) values are between 1 and 10%. (Gr) Gamma-ray, (NEU) neutron log formation, (IK and BK) shallow and deep resistivity. MF 1: peloidal grainstone, MF 2: cemented bioclastic peloidal grainstone, MF 3: echinoderm-concentrated packstone, MF 4: algae packstone, MF 5: bioclastic wackestone, MF6: whole-fossil wackestone, and MF7: dolomites. The locations of the studied wells are shown in Fig. 1D. Track No: 1 presents the depth in meter (measured depth) MD. Track No: 2 presents the (Gr) Gamma-ray and (NEU) neutron log formation. Track No: 3 presents the IK and BK (shallow and deep resistivity). Track No: 4 presents the lithology log from the core description. Track No: 5 presents the porosity from well logs interpretation. Track No: 6 presents the calculated oil saturation. Track No: 7 presents the reservoir or non-reservoir zones. Track No: 8 presents the permeability.

deeper burial environments.

Marine-meteoric mixing zone diagenesis: Paragenetic modifications are typically initiated by the process of sediment deposition in the sedimentary basin and their exposure to varying degrees of bioturbation activities in the near-seafloor diagenetic environment (Flügel, 2010). Micritization, which occurs shortly after deposition, is often recognized as the first diagenetic phase (Flügel, 2004). The presence of micritic envelopes enclosing the allochems, as well as entirely micritized grains (peloids) in MF 1 and MF 2 (see Fig. 3A and B, 5 A, B, D and E), suggests that they were deposited in low-energy settings with restricted grain mobility (Moore and Wade, 2013). Boring by microbes is hypothesized to be the cause of micritization, which occurs during the early phases of diagenesis and impacts bioclasts and carbonate grains (Flügel, 2010; Wang et al., 2021).

The metastable aragonitic skeletal grains are thought to dissolve during the shallow marine burial stage, which occurs at depths of a few meters below the sea floor. This process mostly affects the coarse shell fragments and marine algae, resulting in secondary moldic porosity production (Swei and Tucker, 2012). On the other hand, the common moldic porosity in the Dankovo-Lebedyansky carbonates cannot be explained only by early dissolution. Early dissolution occurred during the early diagenesis stage as a result of subaerial exposure regulated by sea-level changes (Kolchugin et al., 2016, 2020). One of the most notable pieces of evidence suggesting the dominance of dissolution in early diagenesis is that the aragonite bioclastic grains are either partially filled by micro to cryptocrystalline calcite (see Fig. 5B and E; shown by the yellow squares) or empty moulds (see Fig. 7C; indicated by the yellow squares).

In the marine diagenetic environment, carbonate cement precipitation is prevalent following micritization (Flügel, 2010). Early marine cement is interpreted as isopachous rim calcite C1 and bladed rim calcite C2. They represent the first cementation phase by the presence of a high Mg/Ca ratio in the normal seawater. Because of the turbulent bottom currents and the pumping of water with high concentrations of calcium carbonate $CaCO_3$ through the very porous sediments, the carbonate cementing process is most likely to have happened after micritization in the shallow marine diagenetic environment (Moore, 2001). Furthermore, the presence of calcite rims 10 μm thick encircling the allochem grains (see Fig. 5E) supports the shallow marine depositional settings (Zhu et al., 2020).

The selective dolomite D1 that affects several of the examined carbonates, including matrix and grains (see Fig. 6B and C), is comparable to Gregg and Sibley (1984) floating rhombs fabric. It is associated with microfacies deposited on the inner to middle ramp settings (MF 5 and MF 6) and is thought to represent the early stage of dolomitization, suggesting that dolomitization occurred during early diagenesis in low-temperature fluids (Machel, 2004; Al-Qayim et al., 2010; Zhu et al., 2020).

Fabric-selective dissolution occurred during the meteoric diagenetic environment stage, as evidenced by dissolution of the unstable non-skeletal grains such as peloids (see Fig. 3A and B) and skeletal fragments (see Fig. 7B and F) to form moldic pores and vugs that evidence the meteoric diagenetic modifications, which are likely related to sea-level fluctuations, making some microfacies sediments subject to meteoric water impacts (Moore and Wade, 2013; Zhu et al., 2020; Wang et al., 2021).

Drusy calcite C3 and syntaxial calcite C4 are likewise suggested to be precipitated in the meteoric diagenetic environment. The growth and development of C3 and C4 calcites over C1 and C2 calcites, which inhibit their precipitation, gives evidence for this (Flügel, 2010). Dissolution in the meteoric environment affected MF 1 sediments and resulted in creation of the secondary pores (see Fig. 3A and B). However, calcite cementation alters MF 2, resulting in the blocking of the interparticle pores (see Fig. 3C and D).

Shallow-burial diagenetic environment: Mechanical compaction is a crucial event at this stage, as it leads to grain breaking, deformation, and rearrangement (see Fig. 8A, B, and C), as well as microfractures (see Fig. 8H). During the shallow-burial diagenetic stage, the moldic pores formed by fabric-selective dissolution are

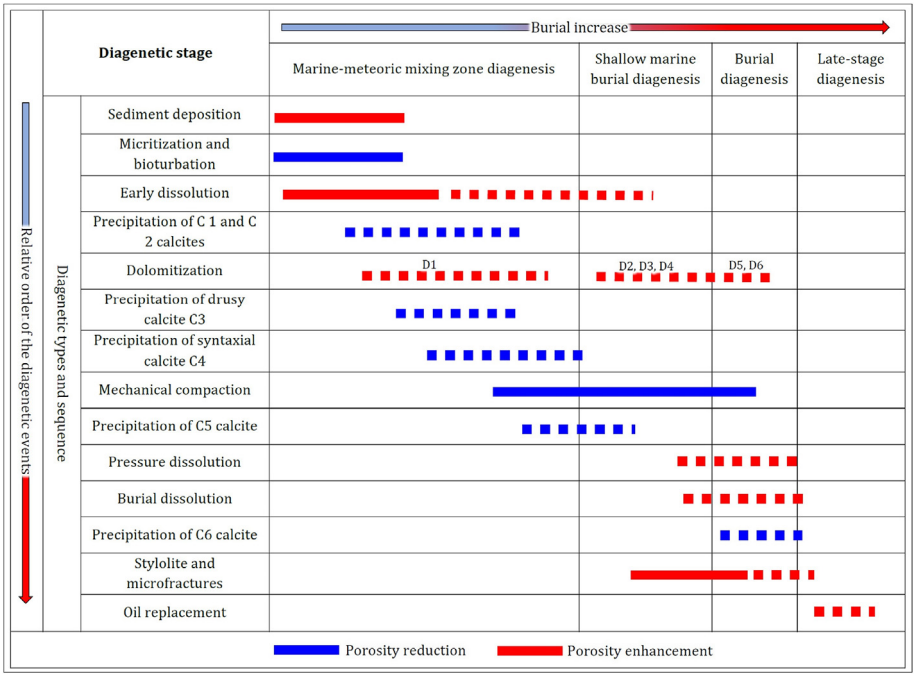

Fig. 11. Representative succession of depositional and diagenetic events as based on the interpretation of data documented in the Dankovo-Lebedyansky sediments.

significantly enlarged, and considerable amounts of C5 cement precipitate, resulting in partial or total filling of the residual pores and secondary moldic pores, as shown in Fig. 5H. Additionally, D2, D3, and D4 dolomites are likely to have developed during shallow burial diagenesis but post-date the submarine calcite cementation (Gregg and Sibley, 1984; Al-Qayim et al., 2010).

Burial and late-stage diagenetic environment: After mechanical compaction established a stable grain framework, the elastic strain on grain contacts increased with progressive burial, resulting in pressure dissolution (Flügel, 2010; Wang et al., 2021) (see Fig. 8F and G). Non-fabric-selective dissolution was observed along stylolites as well as across rock components such as grains and micrite matrix (see Fig. 8H). Because the microfractures were occluded by C6 calcite (see Fig. 5I), it is assumed that they formed prior to C6 precipitation and hydrocarbon charge (Zhu et al., 2020; Wang et al., 2021). As indicated by the thin section investigations presented in Fig. 3C, stylolite and microfractures were also present in the late-stage diagenetic environment.

The widespread dolomite D5, which typically destroys the original fabric and displays an interlocking fabric with a coarsely crystalline mosaic, may indicate that the dolomitization process was late and replacive. The presence of original rock fabric ghosts may suggest that the dolomitizing fluids are Mg^{++} deficient for full dolomitization (Machel, 2004). This type of dolomite's paragenetic relationships and association with the surrounding rocks indicate late diagenetic processes (Sibley, 1982; Al-Qayim et al., 2010). D5 and D6 dolomites are frequently documented as late diagenetic occurrences in deep-burial environments (Gregg and Sibley, 1984; Sibley, 1982; Machel, 2004).

5.2. Control of microfacies on reservoir quality

As previously stated, seven microfacies were identified in the examined Dankovo-Lebedyansky sediments. The pore types differ, resulting in variations in pore network structure and, as a consequence, petrophysical properties; hence, the identified microfacies exhibit a variety of reservoir qualities. Based on petrography, sedimentology, and petrophysical data, the identified microfacies are classified into three distinct classes. The microfacies types with the best reservoir quality are peloidal grainstone MF 1 and dolostone MF 7. Microfacies types of moderate reservoir quality include echinoderm-concentrated packstone MF 3 and algae packstone MF 4. Microfacies types of poor and non-reservoir quality include cemented bioclastic peloidal grainstone MF 2, bioclastic wackestone MF 5, and whole-fossil wackestone MF 6. Each class is described below.

5.2.1. Microfacies types with the best reservoir quality

Thin section investigations of MF 1 revealed significant primary and secondary porosity (Fig. 12A and B). According to Choquette and Pray (1970), the pores between peloid grains are classified as primary interparticle, whereas dissolution pores, vugs, enlarged pores (Fig. 12A; indicated by the red arrows and abbreviated “Por”), or channels along the stylolites are classified as secondary porosity (Fig. 12A; stylolites are indicated by the yellow arrows and abbreviated “Sty”). The pores of MF 1 have a wide range of shapes and sizes (up to 100 μm in diameter and larger when enlarged by dissolution activities), yet they are well-connected, indicating that the pores are permeable despite secondary calcite precipitation (Fig. 12A and B; calcite cement is recognized by the white color on the thin section photomicrography and indicated by the blue arrows and abbreviated “Cal").

Secondary porosity predominates in the dolostone MF 7, shown by the intercrystalline pores between the dolomite crystals, which can reach in size up to 150 μm (Fig. 12C and D; abbreviated “Por”). They are well developed in D3 dolomite (medium crystalline planar-e-s) (Fig. 12C) and D4 dolomite (coarse crystalline planar-e-s) dolomite (Fig. 12D). The porosity between the dolomite crystals was also confirmed to be vuggy or enlarged under the influence of dissolution activities (Fig. 12C; indicated by the red circle). This vuggy porosity is thought to be caused by dolomite crystal partial dissolution during diagenesis (Gregg and Sibley, 1984; Machel, 2004).

5.2.2. Microfacies types with moderate reservoir quality

This type of microfacies is represented by MF 3 and MF 4. The pore network here is formed by interparticle pores and intraparticle micropores as well as dissolution porosity (Fig. 12E and F, respectively). Moldic porosity is the most common in MF 3 and MF 4, and it results from the initial dissolution of the carbonate grains (Ehrenberg et al., 2012). The width of certain moldic pores can expand by 1 mm or more as the dissolution activity increases in association with the partial dissolution of the micritic grains (Fig. 12E; indicated by the red circle). Porosity associated with stylolite may also be found in MF 3 and MF 4. They produce linear and zigzag patterns that connect the pores and, as a result, enhance the porosity and permeability (Fig. 12E; indicated by the yellow arrows). Microscale vugs (cavities or voids less than 1 mm across) are also frequent in MF 3 and MF 4. The principal mechanism for creating them, as indicated by the blue arrows in Fig. 12F, is the dissolution of the original micrite (Ehrenberg et al., 2012).

5.2.3. Microfacies types with poor and non-reservoir quality

MF 2, MF 5, and MF 6 are examples of poor and non-reservoir quality microfacies types. Thin section examinations revealed that in MF 2, extensively calcite cement fills the primary interparticle pores as well as the secondary moldic pores, resulting in total blocking of the pore spaces and porosity and permeability reduction (Fig. 12G; calcite is indicated by the blue arrows and abbreviated “Cal”). Even if certain moldic pores are still partially open and not filled with calcite (Fig. 12G; represented by red arrows and abbreviated “Por”), this does not affect overall porosity or permeability as long as the moldic pores are isolated. The micritic matrix is distributed up to 60% in MF 5 and MF 6 (see Table 1) and forms the majority of the rock components (Fig. 12H and I). Thin section examinations revealed no primary or secondary porosity in MF 5 or MF 6. Dissolution of the skeletal grains was observed and resulted in isolated moldic porosity (Fig. 12H, indicated by the red arrow). However, due to the fact that the moldic pores are isolated and filled by secondary calcite (Fig. 12H, indicated by the blue arrow), it will not enhance the total porosity of the rocks. The occurrence of secondary porosity associated with stylolite microfractures was rarely observed in MF 5 and MF 6. The majority of them are the result of compaction processes that the rocks were subjected to during their burial history (Flügel, 2004). However, because the majority of the stylolites are either filled with mud or have a restricted distribution and low diameters, they do not contribute to the enhancement of the reservoir characteristics of MF 5 and MF 6.

5.3. Control of diagenesis on reservoir quality

Characteristics of the original sedimentary rock texture can be significantly influenced by diagenetic processes. This is determined by the intensity of the carbonate minerals' chemical activity (Tucker, 2001). Petrographic investigation of thin sections indicated that Dankovo-Lebedyansky sediments revealed a variety of diagenetic events such as micritization, cementation, dissolution, and compaction, which influenced the reservoir properties and, as a consequence, enhanced or decreased the pore network.

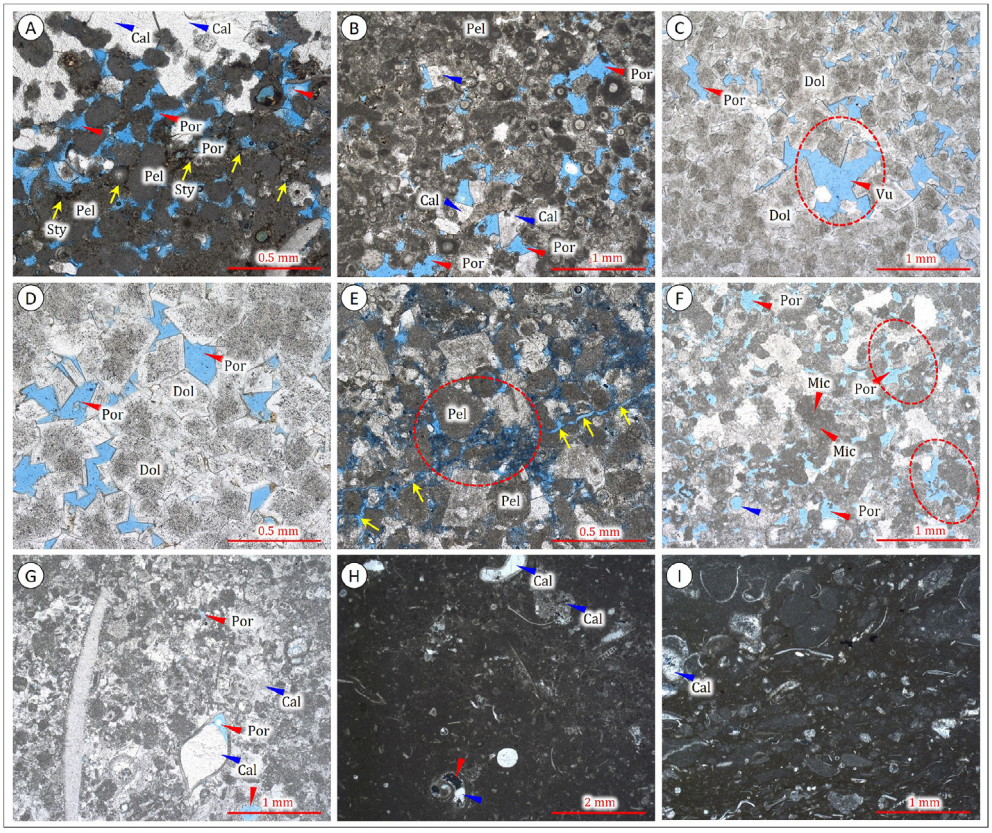

Fig. 12. Representative plane-polarized light (PPL) thin section photomicrographs of the Dankovo-Lebedyansky sediments showing: (A, B) Peloidal grainstone MF 1 dominated by secondary moldic porosity. Calcite cement "Cal" in certain pores. (C) D3 dolomite, well-developed and dominating intercrystalline porosity between dolomite crystals, vuggy porosity up to 150 μm, as shown by the red circle. (D) D4 dolomite, well-developed intercrystalline porosity varying in size from 50 to 100 μm. (E) Echinoderm-concentrated packstone MF 3, developed moldic pores of 1 mm in size, enlarged vugs, and stylolites microfractures also presented. (F) Algae packstone MF 4, moldic and vuggy pores are presented, with patches of secondary calcite filling some of the moldic pores. (G) Cemented bioclastic peloidal grainstone MF 2, the primary and secondary pores are filled with calcite cement "Cal". (H, I) Bioclastic wackestone MF 5 and whole-fossil wackestone MF 6, the micrite fills the bulk of the rock components. No primary or secondary pores were found. Abbreviations: Pel - Peloids; Por - Pores; Sty - Stylolite; Ca - Calcite; Vu - Vugs; Dol - dolomite.

5.3.1. *Effect of micritization*

In general, micritization has a negative impact on reservoir quality attributes. This process assists in the reduction of allochem dissolution and secondary porosity creation. Furthermore, it improves micrite penetration and allochems replacement, which prevents dissolution (Lucia, 2007; Flügel, 2010). On the other hand, micrite envelopes enclosing aragonitic skeletal grains are significant during later diagenesis because they can preserve the grains' form following aragonite dissolution (Lambert et al., 2006).

5.3.2. *Effect of calcite cementation*

Calcite cement, as evidenced by thin section examinations, is presented in all the identified microfacies at rates ranging from 2 to 7% (see Table 1). It is most abundant in the cemented bioclastic peloidal grainstone MF 2, reaching up to 30%. C1, C2, and C3 are the most common calcites in MF 1, which is classified as microfacies with the best reservoir quality. They slightly contribute to reducing the overall porosity and hence permeability by blocking some of the primary and secondary pores. Additionally, the development of calcite crystals on the inner edges of certain pores contributes to the reduction of their diameters and, as a result, their connectivity (Fig. 13A; indicated by the red circle).

Marine cement C1 and C2 are common in MF 2. Herein, the porosity was destroyed (Fig. 12B) as a result of the deposition of this microfacies sediments in the upper inner ramp settings, where high volumes of seawater were flushed into the porous sediments and CO_2 degassing occurred due to high wave or tidal energy (Moore and Wade, 2013). The cementation of MF 2 increased resistance to subsequent compaction during the burial stage, as evidenced by the absence of stylolite or microfractures. Calcite cement also contributes to the reduction of reservoir characteristics in MF 3 (Fig. 12C) and MF 4 (Fig. 12D) by blocking part of the primary and secondary pores, reducing the overall porosity and hence permeability. Calcite is widespread among the components of MF 5 (Fig. 12E) and MF 6 (Fig. 12F), which are primarily classed as non-reservoirs filling the primary and secondary pores and structures of the fossil remains (Fig. 12F; indicated by the red circles).

5.3.3. *Effect of dolomitization*

Overall, the dolomitization process appears to have improved the reservoir properties of the investigated sediments. The formation of oil-saturated intervals, as indicated by the macroscopic evaluation of core samples, confirms this (see Fig. 6A). The D1 dolomite did not significantly improve the reservoir quality because its distribution is selective and confined to certain parts of the matrix or grains (see Fig. 6B and C). D5 and D6 dolomites have contributed to reservoir quality degradation by blocking all pore spaces, owing to an increase in the intensity of the dolomitization process and, as a result, an increase in the precipitation of the dolomite cement between crystals and in the porous spaces (see Fig. 6H and I). D2, as well as D3 and D4 dolomites, have contributed to improving the reservoir quality by forming secondary

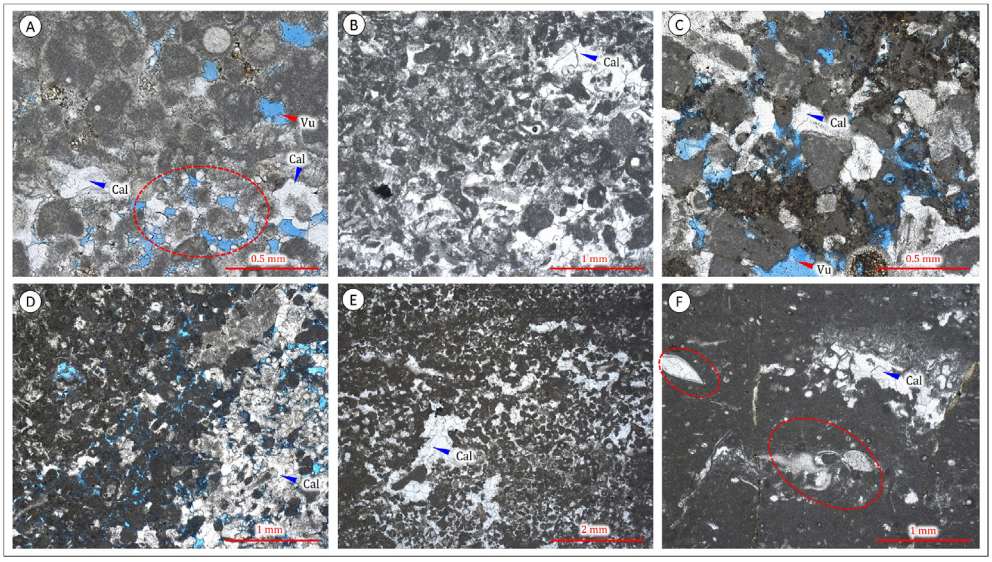

Fig. 13. Representative plane-polarized light (PPL) thin section photomicrographs of the Dankovo-Lebedyansky sediments showing: (A) Patches of calcite cement indicated by the blue arrows and abbreviated "Cal" fills some of the primary and secondary pores in MF 1, newform of calcite cement on the inner edges of some secondary pores indicated by the red circle reduce their diameters and connectivity. (B) Common calcite cement in MF 2 fills the primary and secondary pores. (C) Patches of calcite cement fill some of the remains pores in MF 3. (D) Patches of calcite cement fill some of the remains pores in MF 4. (E) Common calcite cement fills the remains pores in MF 5. (F) Common calcite cement fills the remains pores in MF 6. Abbreviations: Ca - Calcite; Vu - Vugs.

intercrystalline and vuggy porosity with diameters of up to 150 μm (see Figs. 6E and 12C and D).

5.3.4. Effect of dissolution

Dissolution over the various diagenetic events is considered the key process responsible for improving reservoir quality through secondary porosity formation (Flügel, 2004). This is supported by macroscopical investigations of the cored samples as well as thin section examinations, as shown in Fig. 7. Dissolution is the primary source of secondary porosity and reservoir quality enhancement in MF 1. Moldic pores and vugs are formed as a result of the fabric-selective dissolution of the peloids and unstable bioclasts (see Fig. 7B and C). Echinoderms are abundant in MF 3, and its calcite composition is distinguished by chemical stability and resistance to dissolution (Flügel, 2010). As a result, fewer moldic pores were formed (see Fig. 3E). However, the enlargement due to dissolution associated with stylolites increased the porosity and hence the permeability (see Fig. 7E). Furthermore, aragonite-composition algae are common in MF 4. Their metastable composition distinguishes them (Flügel, 2010). This results in the formation of common secondary porosity, as illustrated in Fig. 7F, and explains why the algae in the samples studied were not entirely preserved. Because it is confined to some parts of the micritic matrix and impacts certain of the bioclasts, dissolution did not contribute to improving reservoir quality in MF 2, MF 5, and MF 6. As a result, distributed vuggy porosities occur that are isolated and disconnected (see Fig. 3C, H and I, 7H and I).

5.3.5. Effect of compaction and microfractures

Mechanical compaction, which starts immediately after deposition and continues until chemical compaction takes control, results in rapid loss of porosity in all the identified microfacies. On the other hand, compaction contributed to the formation of microfractures or stylolites, which have a significant influence on the reservoir quality by increasing the permeability of certain microfacies such as MF 1, MF 3, and MF 4 (see Fig. 3E and F, 5C, 7F, 8A, F and H). Compaction does not affect the reservoir quality of MF 2, MF 5, and MF 6 since they are initially classified as microfacies types with poor and non-reservoir quality due to their entirely micritic nature or abundance of calcite cement between their components (see Fig. 3C, D, G, H and I, 8D, E and G).

6. Conclusions

The present study of the Upper Devonian Dankovo-Lebedyansky sediments has resulted in the following conclusions:

(1) Seven microfacies have been identified and clustered into an inner ramp, middle ramp, and outer ramp environments.
(2) The investigated limestones experienced major diagenetic events that affected the reservoir quality. They include micritization, calcite cementation, dolomitization, dissolution, compaction, and microfractures.
(3) Three classes of reservoir quality were recognized based on petrophysical characterization of the identified microfacies. MF 1 and MF 7 are microfacies with the best reservoir quality. MF 3 and MF 4 are microfacies with moderate reservoir quality. MF 2, MF 5, and MF 6 are microfacies with poor and non-reservoir reservoir quality.
(4) Calcite cementation, micritization, and compaction are among the main reasons that led to losing the initial porosity of the sediment at the early stage of the diagenetic history, while dissolution led to formation of the secondary moldic pores, which eventually led to an increase in the overall porosity.
(5) Dolomitization, stylolite, and microfractures may have increased porosity locally as well by creating intercrystalline, channels, or vuggy porosity.
(6) The concepts concluded in this study provide a typical case where reservoir quality is jointly controlled by sedimentary facies variation and diagenetic modifications. Understanding

this interaction can help in understanding the behavior of similar reservoirs in the area.

Declaration of competing interest

On behalf of all the co-authors, the corresponding author states that there is no conflict of interest.

Acknowledgments

This work was supported by the Ministry of Science and Higher Education of the Russian Federation under agreement No. 075-15-2022-299 within the framework of the development program for a world-class Research Center “Efficient development of the global liquid hydrocarbon reserves”. The authors acknowledge the constructive comments of the anonymous reviewers, the associate editor, and the journal editor-in-chief Dr. Chengzao Jia.

References

Abdel-Fattah, M.I., Mahdi, A.Q., Theyab, M.A., Pigott, J.D., Abd-Allah, Z.M., Radwan, A.E., 2022. Lithofacies classification and sequence stratigraphic description as a guide for the prediction and distribution of carbonate reservoir quality: a case study of the Upper Cretaceous Khasib Formation (East Baghdad oilfield, central Iraq). J. Petrol. Sci. Eng. 209, 109835.

Abdullah, G.M.S., El Aal, A.A., Radwan, A.E., Qadri, T., Aly, Nevin, 2022. The influence of carbonate textures and rock composition on durability cycles and geo-mechanical aspects of carbonate rocks. Acta Geotechnica 1–21.

Ahmad, F., Quasim, M.A., Ahmad, A.H.M., 2021. Microfacies and diagenetic over-prints in the limestones of middle jurassic fort member (jaisalmer formation), western Rajasthan, India: implications for the depositional environment, cyclicity, and reservoir quality. Geol. J. 56 (1), 130–151.

Ahr, W.M., 2008. Geology of Carbonate Reservoirs: the Identification, Description, and Characterization of Hydrocarbon Reservoirs in Carbonate Rocks. Wiley, New York, pp. 130–150.

Al-Qayim, B., Qadir, F.M., Albeyati, F., 2010. Dolomitization and porosity evaluation of the cretaceous upper qamchuqa (mauddud) formation, khabbaz oil field, kirkuk area, northern Iraq. GeoArabia 15 (4), 49–76.

Bjørlykke, K., 2014. Relationships between depositional environments, burial history and rock properties. Some principal aspects of diagenetic process in sedimentary basins. Sediment. Geol. 301, 1–14.

Boutaleb, K., Baouche, R., Sadaoui, M., Radwan, A.E., 2022. Sedimentological, petrophysical, and geochemical controls on deep marine unconventional tight limestone and dolostone reservoir: insights from the Cenomanian/Turonian oceanic anoxic event 2 organic-rich sediments, Southeast Constantine Basin, Algeria. Sediment. Geol. 429, 106072.

Burchette, T.P., 2012. Carbonate rocks and petroleum reservoirs: a geological perspective from the industry. Geological Society, London, Special Publications 370 (1), 17–37.

Choquette, P.W., Pray, L.C., 1970. Geologic nomenclature and classification of porosity in sedimentary carbonates. AAPG Bull. 54 (2), 207–250.

Dunham, R.J., 1962. Classification of carbonate rocks according to depositional texture. In: Ham, W.E. (Ed.), Classification of Carbonate Rocks, vol. 1. AAPG Memoir, pp. 108–121.

Ehrenberg, S.N., Nadeau, P.H., 2005. Sandstone vs. carbonate petroleum reservoirs: a global perspective on porosity-depth and porosity-permeability relationships. AAPG (Am. Assoc. Pet. Geol.) Bull. 89 (4), 435–445.

Ehrenberg, S.N., Walderhaug, O., Bjørlykke, K., 2012. Carbonate porosity creation by mesogenetic dissolution: reality or illusion? AAPG Bull. 96, 217–233.

Flügel, E., 2004. Microfacies of Carbonate Rocks, Analysis, Interpretation and Application. Springer – Verlag, New York.

Flügel, E., 2010. Microfacies of Carbonate Rocks: Analysis, Interpretation and Application, second ed. Springer, Heidelberg Dordrecht London, New York, p. 984.

Folk, R.L., 1959. Practical petrographic classification of limestones. AAPG Bull. 43, 1–38.

Galimov, E.M., Kamaleeva, A.I., 2015. Hydrocarbon source of the super-giant oil field Romashkino (Tatarstan) - tributary from the crystalline basement or source material sedimentary deposits. Geochemistry 2, 103–122.

Gregg, J.M., Sibley, D.F., 1984. Epigenetic dolomitization and the origin of xenotopic dolomite texture. J. Sediment. Res. 54, 908–931.

Ibrahem, Y., Morozov, V.P., Sudakov, V., Idrisov, I., Kolchugin, A.N., 2022b. Sedimentary diagenesis and pore characteristics for the reservoir evaluation of Domanik formations (Semiluksk and Mendymsk) in the central part of Volga-Ural petroleum province. Petroleum Research 7 (1), 32–46.

Ibrahem, Y., Morozov, V.P., Sudakov, V., Idrisov, I., Kolchugin, A.N., Leontev, A., 2022a. Microfacies analysis and depositional environment of the upper devonian dankovo-lebedyansky sediments, tatarstan, Volga-Ural Basin, Russia. Petroleum Research. https://doi.org/10.1016/j.ptlrs.2022.07.003 (in press).

Kerimov, V.Y., Osipov, A.V., Lavrenova, E.A., 2014. The hydrocarbon potential of deep horizons in the south-eastern part of the Volga-Urals oil and gas province. Neft. Khozyaystvo Oil Ind. 4, 33–35.

Klett, T.R., Brownfield, M.E., Finn, T.M., Gaswirth, S.B., Le, P.A., Leathers-Miller, H.M., Marra, K.R., Mercier, T.J., Pitman, J.K., Schenk, C.J., Tennyson, M.E., Woodall, C.A., 2018. Assessment of undiscovered continuous oil and gas resources in the Domanik-type formations of the Volga-Ural Region Province, Russia, 2017. U.S. Geol. Surv. Fact Sheet. 2. https://doi.org/10.3133/fs20173085.

Kolchugin, A., Immenhauser, A., Morozov, V., Walterc, B., Eskin, Aleksey, Korolev, E., Neuser, R., 2020. A comparative study of two Mississippian dolostone reservoirs in the Volga-Ural Basin, Russia. J. Asian Earth Sci. 199, 104465.

Kolchugin, A.N., Immenhauser, A., Walter, B.F., Morozov, V.P., 2016. Diagenesis of the palaeo-oil-water transition zone in a Lower Pennsylvanian carbonate reservoir: constraints from cathodoluminescence microscopy, microthermometry, and isotope geochemistry. Mar. Petrol. Geol. 72, 45–61.

Korshunov, D.M., Boguslavskiy, M.A., 2022. Mineralogical–Geochemical features, genesis, and age of refractory clays in the shulepovo deposit (ryazan region, central European Russia). Lithol. Miner. Resour. 57 (1), 78–94.

Lai, J., Wang, G., Chai, Y., Xin, Y., Wu, Q., Zhang, X., Sun, Y., 2017. Deep burial diagenesis and reservoir quality evolution of high-temperature, high-pressure sandstones: examples from Lower Cretaceous Bashijiqike Formation in Keshen area, Kuqa depression, Tarim basin of China. AAPG (Am. Assoc. Pet. Geol.) Bull. 101 (6), 829–862.

Lai, J., Wang, G., Wang, S., Cao, J., Li, M., Pang, X., Zhou, Z., Fan, X., Dai, Q., Yang, L., He, Z., Qin, Z., 2018. Review of diagenetic facies in tight sandstones: diagenesis, diagenetic minerals, and prediction via well logs. Earth Sci. Rev. 185, 234–258.

Lambert, L., Durlet, Ch, Loreau, J.P., Marnier, G., 2006. Burial dissolution of micrite in Middle East carbonate reservoirs (Jurassic–Cretaceous): keys for recognition and timing. Mar. Petrol. Geol. 23, 79–92.

Liang, X.P., Galushyn, G.A., Filippov, V.P., 2015. Conditions of domanicites formation in the south-eastern part of the Russian platform. Georesursy 3 (62), 54–63.

Liang, X.P., Jin, Z.J., Alexander, S., Yin, J.Y., Liu, Q.Y., Uspensky, B., 2019. Geological characteristics and latest progress in exploration and development of Russian shale oil. Oil Gas Geol. 40 (3), 478–490.

Liang, X.P., Jin, Z.J., Philippov, V., Obryadchikov, O., Zhong, D.K., Liu, Q.Y., Uspensky, B., Morozov, V., 2020. Sedimentary characteristics and evolution of domanik facies from the devonian–carboniferous regression in the southern Volga-Ural Basin. Mar. Petrol. Geol. 119, 104438.

Liu, H., Shi, K., Liu, B., Song, X., Guo, R., Wang, G., Wang, H., 2021. Microfacies and reservoir quality of the middle cretaceous rumaila formation in the AD oilfield, central mesopotamian basin, southern Iraq. J. Asian Earth Sci. 213, 104726.

Longman, M.W., 1980. Carbonate diagenetic textures from nearsurface diagenetic environments. AAPG Bull. 64 (4), 461–487.

Lucia, F.J., 1995. Rock-fabric/petrophysical classification of carbonate pore space for reservoir characterization. AAPG Bull. 79, 1275–1300.

Lucia, F.J., 2007. Carbonate Reservoir Characterization, second ed. Springer-Verlag, Berlin, pp. 236–270.

Machel, H.G., 2004. Concept and models of dolomitization: a critical reappraisal. In: Braithwaite, C.J., Rizzi, G., Darke, G. (Eds.), The Geometry and Petrophysics of Dolomite Hydrocarbon Reservoir, vol. 235. Geological Society of London Special Publication, pp. 7–63.

Moore, C.H., 2001. Carbonate Reservoirs: Porosity Evolution and Diagenesis in a Sequence Stratigraphic Framework. Elsevier, Amsterdam, pp. 450–480.

Moore, C.H., Wade, W.J., 2013. Carbonate reservoirs porosity and diagenesis in a sequence stratigraphic framework. Dev. Sedimentol. 67, 1–374.

Morozov, V.P., Jin, Z.J., Liang, X.P., Korolev, E.A., Liu, Q.Y., Kolchugin, A.N., Eskin, A.A., Nizamova, A.V., Assumption, B.V., Liu, G.X., 2021. Comparison of source rocks from the lower silurian longmaxi formation in the yangzi Platform and the Upper Devonian Semiluksk Formation in east European Platform. Energy Geosci. 2, 63–72.

Mukhametdinova, A., Kazak, A., Karamov, T., Bogdanovich, N., Melekhin, S., Cheremisin, A., 2020. Reservoir properties of low-permeable carbonate rocks: experimental features. Energies 13 (9), 2233.

Noel, P.J., Brian, J., 2015. The Origin of Carbonate Sedimentary Rocks. American Geophysical Union, Wiley works, p. 464p.

Radwan, A.E., Trippetta, F., Kassem, A.A., Kania, M., 2021. Multi-scale characterization of unconventional tight carbonate reservoir: insights from October oil filed, Gulf of Suez rift basin, Egypt. J. Petrol. Sci. Eng. 197, 107968.

Sibley, D.F., 1982. The origin of common dolomite fabrics. J. Sediment. Petrol. 52, 1987–2100.

Sibley, D.F., Gregg, J.M., 1987. Classification of dolomite rock texture. J. Sediment. Petrol. 57, 967–975.

Smirnov, M.B., Borisov, R.S., Fadeeva, N.P., Poludetkina, E.N., 2018. The characteristics of the organic matter of the upper devonian domanik-type deposits in the northern and central regions of the Volga-Ural Basin according to saturated biomarkers composition. Geochem. Int. 56 (8), 812–827.

Strakhov, N.M., 1939. Доманиковая фация ЮЖного Урала [Текст]. In: Proceedings of the Institute of Geological Sciences, vol. 6. Academy of Sciences of the USSR, Moscow (Dnepropetrovsk), p. 122.

Swei, G.H., Tucker, M.E., 2012. Impact of diagenesis on reservoir quality in ramp carbonates: gialo formation (Middle Eocene), Sirt Basin, Libya. J. Petrol. Geol. 35 (1), 25–47.

Tucker, M.E., 2001. Sedimentary Petrology: an Introduction to the Origin of Sedimentary Rocks. Blackwell, Scientific Publication, London.

Tucker, M.E., Wright, V.P., 1990. Carbonate Sedimentology. Blackwell, London,

pp. 470–490.
Wang, H., Shi, K., Ma, Y., Liu, B., Song, X., Ge, Y., Liu, H., Hoffmann, R., Immenhauser, A., 2021. Control of depositional and diagenetic processes on the reservoir properties of the Mishrif Formation in the AD oilfield, Central Mesopotamian Basin, Iraq. Mar. Petrol. Geol. 132, 105202.
Worden, R.H., Armitage, P.J., Butcher, A.R., Churchill, J.M., Csoma, A.E., Hollis, C., Lander, R.H., Omma, J.E., 2018. Petroleum reservoir quality prediction: overview and contrasting approaches from sandstone and carbonate communities. Geological Society, London, Special Publications 435 (1), 1–31.
Zhu, X., Jin, Z., Liang, T., Yi, S., Wei, K., Gao, B., Shi, L., 2020. Depositional environment, diagenetic evolution, and their impact on the reservoir quality of the carboniferous KT-II carbonate in the zhanazhol reservoir, Pre-Caspian Basin, Kazakhstan. Mar. Petrol. Geol. 117, 104411.